

Optimal Bayesian Design for Model Discrimination via Classification

Markus Hainy^{1,2}, David J. Price^{3,4,5}, Olivier Restif⁵, and Christopher Drovandi^{1,6}

¹School of Mathematical Sciences, Queensland University of Technology, Brisbane QLD 4000, Australia

²Department of Applied Statistics, Johannes Kepler University, 4040 Linz, Austria

³Centre for Epidemiology and Biostatistics, Melbourne School of Population and Global Health, The University of Melbourne, VIC 3010, Australia

⁴Victorian Infectious Diseases Reference Laboratory Epidemiology Unit, The Peter Doherty Institute for Infection and Immunity, The University of Melbourne, Royal Melbourne Hospital, VIC 3000, Australia

⁵Department of Veterinary Medicine, University of Cambridge, Cambridgeshire CB3 0ES, United Kingdom

⁶ARC Centre of Excellence for Mathematical & Statistical Frontiers

December 15, 2024

Abstract

Performing optimal Bayesian design for discriminating between competing models is computationally intensive as it involves estimating posterior model probabilities for thousands of simulated datasets. This issue is compounded further when the likelihood functions for the rival models are computationally expensive. A new approach using supervised classification methods is developed to perform Bayesian optimal model discrimination design. This approach requires considerably fewer simulations from the candidate models than previous approaches using approximate Bayesian computation. Further, it is easy to assess the performance of the optimal design through the misclassification matrix. The approach is particularly useful in the presence of models with intractable likelihoods but can also provide computational advantages when the likelihoods are manageable.

Keywords: Simulation-based Bayesian experimental design, approximate Bayesian computation, model selection, classification, machine learning, classification and regression tree, random forest, continuous-time Markov process, spatial extremes

1 Introduction

In many applications, finding the most appropriate model among a class of possible models is an important goal of statistical inference. In the classical literature, these decisions are commonly based on model selection criteria such as the Akaike information criterion or related

criteria (Konishi and Kitagawa, 2008). The Bayesian approach, where the model indicator is regarded as an additional unknown random variable, offers a coherent decision-theoretic framework for inference and model discrimination (Key et al., 1999). Common options to carry out model selection in a Bayesian context are Bayes factors (Kass and Raftery, 1995), the deviance information criterion (Spiegelhalter et al., 2002), or the computation of the marginal likelihoods or evidence (Friel and Pettitt, 2008). Given the prior model probabilities, the marginal likelihoods can be turned into posterior model probabilities. Classical model selection criteria only provide a ranking of the models, whereas posterior model probabilities contain useful information about the likelihoods of the various models as well. In addition, the posterior model probabilities may also be incorporated in predictive inference.

In optimal experimental design, one seeks to find the optimal combination of the controllable factors in order to maximise the (expected) information gain of the experiment (Atkinson et al., 2007). For the experimental goal of model discrimination, the most commonly used classical design criterion is T-optimality (Atkinson and Federov, 1975a,b; Dette and Titoff, 2009), with extensions to Bayesian T-optimality (Ponce de Leon and Atkinson, 1992) to incorporate prior information. Except for robust T-optimal designs (Vajjah and Duffull, 2012), one model has to be selected which is assumed to be the true model. Furthermore, T-optimal designs are generally computationally expensive.

Fully Bayesian experimental design provides a consistent framework to handle parameter and model uncertainty when planning the experiment (Chaloner and Verdinelli, 1995; Ryan et al., 2016). For model discrimination, the most popular design criterion is the mutual information between the model indicator and the data, which is measured by the Kullback-Leibler divergence between the joint and marginal distributions of those two random variables (see Box and Hill (1967)). This criterion requires the computation of the evidence of each model for many potential observations, so its use has been confined to a limited set of applications such as simple models with conjugate priors (Ng and Chick, 2004), cases where numerical quadrature is feasible (Cavagnaro et al., 2010), or sequential design settings (Drovandi et al., 2014a). Overstall et al. (2018a) employ normal-based approximations to find optimal designs for several criteria including mutual information and misclassification error. Dehideniya et al. (2018) use approximate Bayesian computation (ABC) to estimate these criteria for intractable epidemiological Markov process models. The ABC approach only requires the ability to simulate from all the candidate models. However, their approach is simulation- and memory-intensive and is thus limited to low-dimensional designs.

Like Dehideniya et al. (2018), we suggest a simulation-based approach. However, we use the outputs of standard supervised classification procedures from machine learning (see Hastie et al. (2009)) to estimate the design criteria. In particular, we employ classification trees (Breiman et al., 1984) and random forests (Breiman, 2001). We demonstrate that this approach considerably reduces the required number of simulations compared to ABC. In order to keep the computational burden manageable, Dehideniya et al. (2018) pre-simulate a large sample from the prior predictive distribution at a grid of possible design points and re-use these simulations for all the designs they consider during the optimisation process, refining the grid over time. However, as we require less simulations for the classification approach, it is not necessary to pre-simulate the data. As a consequence, the classification approach is much more flexible and suitable for much higher-dimensional designs. Furthermore, the classification approach does not require direct approximations of posterior quantities such as the posterior model

probabilities, which may only be reliably estimated with great computational effort, making it a viable alternative for many models with tractable likelihoods. Another advantage of the classification approach is that one can readily use the output from the classification procedures to assess the designs by estimating misclassification error rates or misclassification matrices. Our method represents the first machine learning approach for optimal Bayesian design.

Section 2 reviews Bayesian experimental design and the associated expected utility and loss functions. Our classification approach is presented in Section 3 along with a discussion of classification and regression trees (CART) and random forests. In Section 4, we provide three examples to demonstrate the utility of the classification approach: discriminating between the epidemiological Markov process models of the same type as considered by Dehideniya et al. (2018) (Section 4.1), discriminating between three Markov process models describing the dynamics of bacteria within phagocytic cells (Section 4.2), and discriminating between three spatial extremes models (Section 4.3). In addition, Appendix B contains a logistic regression example considered previously (e.g., Overstall et al. (2018a)). A description of the modified coordinate exchange algorithm that we employ for all our examples can be found in Appendix A. Appendices C – G contain additional results for the examples in Section 4.

2 Optimal Bayesian Design for Model Discrimination

We assume there are K candidate statistical models for a process of interest, one of them being the true underlying model. The models are indexed by the model indicator random variable $M \in \{1, 2, \dots, K\}$. Each model $M = m$ has a likelihood function $p(\mathbf{y}|\boldsymbol{\theta}_m, m, \mathbf{d})$, with data $\mathbf{y} \in \mathcal{Y}$, and parameter vector $\boldsymbol{\theta}_m \in \Theta_m$. In the experimental design context, the likelihood depends on the design vector $\mathbf{d} \in \mathcal{D}$, which is a vector of controllable variables of the experiment that might influence the informativeness of the data \mathbf{y} . In the Bayesian framework, a prior distribution $p(\boldsymbol{\theta}_m|m)$ is assigned to the parameters of each model m . Furthermore, we assign a prior probability $p(m)$ to each model such that $\sum_{m=1}^K p(m) = 1$.

Optimal experimental design requires the specification of a design criterion that encodes the goal of the experiment. In Bayesian design, a function l that quantifies the loss of an experiment needs to be specified, see, e.g., Overstall et al. (2018a). Apart from the design \mathbf{d} , this loss function usually also depends on the model indicator m and the data \mathbf{y} observed at the experiment. It may also depend on the parameters $\boldsymbol{\theta}_m$ at each of the models. For experimental design, the expected or integrated loss,

$$l(\mathbf{d}) = \mathbb{E}_{\boldsymbol{\theta}_m, \mathbf{y}, M|\mathbf{d}}[l(\mathbf{d}, \boldsymbol{\theta}_m, \mathbf{y}, M)],$$

is of interest, where the expectation is taken with respect to all the unknown variables. The optimal design is given by $\mathbf{d}^* = \arg \min_{\mathbf{d} \in \mathcal{D}} l(\mathbf{d})$, where \mathcal{D} is the set of admissible designs, which in general is a challenging optimisation problem. Alternatively, the design problem may be formulated in terms of a utility function instead of a loss function. Then the goal is to maximise the expected utility function.

In Bayesian model discrimination, we are interested in finding a design \mathbf{d} that is likely to produce data \mathbf{y} from which we can infer the posterior distribution of the model indicator M with minimal uncertainty. The most popular measure of uncertainty of a distribution is its

Shannon entropy (see, e.g., Lindley (1956)). For a given dataset \mathbf{y} , the conditional entropy of the model indicator is given by

$$l_{MD}(\mathbf{d}, \mathbf{y}) = - \sum_{m=1}^K p(m|\mathbf{y}, \mathbf{d}) \log p(m|\mathbf{y}, \mathbf{d}).$$

The conditional entropy features the loss function

$$l_{MD}(\mathbf{d}, \mathbf{y}, m) = -\log p(m|\mathbf{y}, \mathbf{d}),$$

which is called the *multinomial deviance loss* (Hastie et al., 2009).

Since \mathbf{y} is not known in advance, we take the average over the marginal distribution of \mathbf{y} , $p(\mathbf{y}|\mathbf{d})$. For continuous data \mathbf{y} , the expected multinomial deviance loss is

$$l_{MD}(\mathbf{d}) = - \int_{\mathbf{y}} p(\mathbf{y}|\mathbf{d}) \sum_{m=1}^K p(m|\mathbf{y}, \mathbf{d}) \log p(m|\mathbf{y}, \mathbf{d}) d\mathbf{y}.$$

Using Bayes rule we can re-write this as

$$l_{MD}(\mathbf{d}) = - \sum_{m=1}^K p(m) \int_{\mathbf{y}} p(\mathbf{y}|m, \mathbf{d}) \log p(m|\mathbf{y}, \mathbf{d}) d\mathbf{y}. \quad (2.1)$$

The negative of the expected multinomial deviance loss is also known as the *mutual information utility* (see, e.g., Drovandi et al. (2014a)).

Another common loss function for model discrimination is the *0–1 loss* (Devroye et al., 1996; Rose, 2008; Overstall et al., 2018a). Let $\hat{m}(\mathbf{y}|\mathbf{d})$ be a classifier function that assigns one of the class labels $1, \dots, K$ to the data \mathbf{y} . The 0–1 loss function is defined as

$$l_{01}(\mathbf{d}, \mathbf{y}, m) = \mathbb{I}[\hat{m}(\mathbf{y}|\mathbf{d}) \neq m] = 1 - \mathbb{I}[\hat{m}(\mathbf{y}|\mathbf{d}) = m],$$

where $\mathbb{I}[\cdot]$ is the indicator function, which takes the value 1 if the argument is true and 0 otherwise. Therefore, the 0–1 loss is 1 if the data is misclassified and 0 if it is classified correctly. A generalisation of this loss function would be a loss matrix that assigns different loss values to all the combinations of true and selected models. Integrating the 0–1 loss function over the prior predictive distribution of the data and the model indicators yields the *misclassification error rate* or *prior error rate* (Pudlo et al., 2016),

$$\begin{aligned} l_{01}(\mathbf{d}) &= \int_{\mathbf{y}} p(\mathbf{y}|\mathbf{d}) \sum_{m=1}^K p(m|\mathbf{y}, \mathbf{d}) \{1 - \mathbb{I}[\hat{m}(\mathbf{y}|\mathbf{d}) = m]\} d\mathbf{y} \\ &= \int_{\mathbf{y}} p(\mathbf{y}|\mathbf{d}) \{1 - p[\hat{m}(\mathbf{y}|\mathbf{d})|\mathbf{y}, \mathbf{d}]\} d\mathbf{y}. \end{aligned} \quad (2.2)$$

The classifier $\hat{m}(\mathbf{y}|\mathbf{d}) = \arg \max_{m \in \{1, \dots, K\}} p(m|\mathbf{y}, \mathbf{d})$ – also known as the *Bayes classifier* – classifies the data according to the posterior modal model. It can be shown that the Bayes classifier minimises the expected 0–1 loss (2.2). The misclassification error rate for the Bayes classifier is called the *Bayes error rate* (see Hastie et al. (2009)).

Unfortunately, the integrals in Equations (2.1) and (2.2) can be high-dimensional, analytically intractable and computationally intensive to approximate accurately. One approach is to estimate them using Monte Carlo integration. Let $\mathbf{y}^{m,j} \sim p(\mathbf{y}|m, \mathbf{d}) = \int_{\boldsymbol{\theta}_m} p(\mathbf{y}|\boldsymbol{\theta}_m, m, \mathbf{d}) p(\boldsymbol{\theta}_m|m) d\boldsymbol{\theta}_m$ for $j = 1, \dots, J$ and $m = 1, \dots, K$. That is, the $\mathbf{y}^{m,j}$ are drawn from the prior predictive distribution under each of the models, in turn. Then we can estimate the expected loss (2.1) by

$$\hat{l}_{MD}(\mathbf{d}) = - \sum_{m=1}^K p(m) \frac{1}{J} \sum_{j=1}^J \log p(m|\mathbf{y}^{m,j}, \mathbf{d}), \quad (2.3)$$

and the expected loss (2.2) by

$$\hat{l}_{01}(\mathbf{d}) = 1 - \sum_{m=1}^K p(m) \frac{1}{J} \sum_{j=1}^J \mathbb{I}[\hat{m}(\mathbf{y}^{m,j}|\mathbf{d}) = m], \quad (2.4)$$

respectively, where $\hat{m}(\mathbf{y}^{m,j}|\mathbf{d}) = \arg \max_{m \in \{1, \dots, K\}} p(m|\mathbf{y}^{m,j}, \mathbf{d})$.

The first issue with these approximations is that J may need to be large to estimate the expected loss with low variance. The second issue is that the posterior model probability, $p(m|\mathbf{y}, \mathbf{d})$, is generally not available analytically and is difficult to approximate accurately. In fact, estimating this quantity is a research problem in its own right in the Bayesian community (Friel and Wyse, 2012). Further complications arise for estimating $p(m|\mathbf{y}, \mathbf{d})$ when the likelihood function $p(\mathbf{y}|\boldsymbol{\theta}_m, m, \mathbf{d})$ for the models of interest is computationally intractable (see, e.g., Dehideniya et al. (2018)). In the Bayesian optimal design setting, an estimate of the expected loss requires $K \times J$ evaluations/approximations of $p(m|\mathbf{y}, \mathbf{d})$ for many different datasets \mathbf{y} . Then, the expected loss must be optimised over a potentially large design space \mathcal{D} , and therefore many thousands of posterior model probabilities must be calculated to arrive at an optimal design. This is why only relatively simple models have been considered in the Bayesian design literature for model discrimination in comparison to the elaborate models that can be analysed in Bayesian inference (see, e.g., the application in Drovandi et al. (2014b)). The ultimate goal of this paper to help bridge this gap.

There have been previous attempts in the literature to estimate the mutual information utility for model discrimination. Ng and Chick (2004) use conjugate priors so that integrals can be computed analytically. Cavagnaro et al. (2010) use quadrature, which suffers from the curse of dimensionality. In a sequential experimental design context, Drovandi et al. (2014a) use sequential Monte Carlo to efficiently and conveniently estimate the posterior model probabilities. However, their approach is only suitable in a sequential design context, where the number of design variables considered for each new data batch is very small. Another approach is to use crude approximations of posterior model probabilities. For example, Overstall et al. (2018a) consider Gaussian-based posterior approximations in order to compute the expected loss estimates (2.3) and (2.4). However, the accuracy of their expected loss estimates depends on the similarity of the posterior distributions to a normal distribution. Dehideniya et al. (2018) tackle the problem of Bayesian model discrimination for models with intractable likelihoods. They use an ABC approach to estimate the posterior model probabilities, which is essentially an extension of the ABC design approach of Drovandi and Pettitt (2013) for parameter estimation. There are several drawbacks of the ABC approach of Dehideniya et al. (2018) that our classification method overcomes, which we discuss further in Section 4.1.

3 The Classification Approach

3.1 Methodology

In this paper we take a classification perspective on the Bayesian model discrimination problem to greatly reduce the computational burden highlighted in the previous section. As a by-product, we also obtain several other advantages over the standard Bayesian approach. The only requirement to apply our methodology is that it is computationally efficient to simulate from each of the K models. Therefore, the class of models that can be considered in optimal design for model selection increases dramatically. In addition, the generality of the proposed approach allows for implementations that are less application-specific. Furthermore, we find that the performance of the optimal design can be assessed easily via the misclassification matrix, as opposed to performing more posterior calculations at the optimal and sub-optimal designs.

For each design \mathbf{d} proposed in the design optimisation algorithm, our approach involves simulating J samples from the joint distribution of data and model indicators,

$$p(\mathbf{y}, m | \mathbf{d}) = \int_{\boldsymbol{\theta}_m} p(\mathbf{y} | \boldsymbol{\theta}_m, m, \mathbf{d}) p(\boldsymbol{\theta}_m | m) p(m) d\boldsymbol{\theta}_m,$$

to generate the training sample $\mathcal{T} = \{m^j, \mathbf{y}^j\}_{j=1}^J$.

We can use this training sample to train a supervised classification algorithm, where we consider the model indicator m as a categorical response or ‘target’ variable and the simulated data \mathbf{y} as the features. As a result, we obtain a classifier function $\hat{m}_C(\mathbf{y} | \mathbf{d}, \mathcal{T})$ that we can use in Equation (2.4) instead of the Bayes classifier to estimate the misclassification error rate. More specifically, if $\mathcal{T}_* = \{m_*^j, \mathbf{y}_*^j\}_{j=1}^{J_*}$ is another independent sample from the distribution $p(\mathbf{y}, m | \mathbf{d})$ of size J_* , we can estimate the misclassification error rate (2.2) as

$$\hat{l}_{01}(\mathbf{d}) = 1 - \frac{1}{J_*} \sum_{j=1}^{J_*} \mathbb{I}[\hat{m}_C(\mathbf{y}_*^j | \mathbf{d}, \mathcal{T}) = m_*^j]. \quad (3.1)$$

Larger values of J and J_* allow for a more accurate estimate of the misclassification error rate, and therefore lead to a less noisy objective function to optimise over, although the time to estimate the error rate increases. However, for intractable likelihood models the sample sizes J and J_* needed for the classification approach to obtain a reasonably precise approximation of the expected loss function are several orders of magnitude less than the sample sizes required for ABC (Pudlo et al., 2016). Moreover, for many other models the classification approach may be more time-efficient than estimating $p(m | \mathbf{y}, \mathbf{d})$ in a conventional way.

If the classification method has a built-in mechanism to correct for overfitting or there is only moderate overfitting, one may avoid generating the test sample \mathcal{T}_* and use the training sample \mathcal{T} instead of \mathcal{T}_* in Equation (3.1). Even if overfitting is present and the misclassification error rates for all the designs are therefore underestimated, there will be no effect on the optimal design if the ranking of the designs is not affected.

Many classification methods also provide estimates of the posterior model probabilities, $\hat{p}_C(m | \mathbf{y}, \mathbf{d}, \mathcal{T})$, which can be used to estimate the expected multinomial deviance loss (2.1) in

a similar way as the misclassification error rate is estimated by Equation (3.1). However, the estimates for the posterior model probabilities provided by many computationally efficient methods such as classification trees or linear discriminant analysis are rather crude, noisy and biased.

Even if the posterior model probabilities are estimated poorly, the classification method can perform quite well at the task of assigning the correct class labels to the observations. All that matters is that the posterior modal model is identified correctly. If a classifier assigns the posterior modal model $\arg \max_m p(m|\mathbf{y}, \mathbf{d})$ to each dataset $\mathbf{y} \in \mathcal{Y}$, it is called an *order-correct classifier* (Breiman, 1996). For an order-correct classifier, the misclassification error rate corresponds to the Bayes error rate and is therefore minimal. The misclassification error rate of a classifier that is order-correct everywhere except for a small subset of the sample space \mathcal{Y} will still be very close to the Bayes error rate. Therefore, the misclassification error rate is relatively robust to inaccurate estimates of the posterior model probabilities. For this reason we focus mainly on finding designs which are optimal with respect to the misclassification error rate.

It is also possible to use a summary of the data, $\mathbf{s}(\mathbf{y})$, as the set of features, where $\mathbf{s}(\cdot)$ is a function that projects the dataset \mathbf{y} onto a lower-dimensional space. Some classification methods may perform better with a smaller number of features. However, as noted by Robert et al. (2011), an inappropriate choice of summary statistics can amount to a significant loss of information regarding model discrimination, even in the limit as the sample size goes to infinity. Generally speaking, identifying summary statistics useful for model discrimination is not intuitive.

3.2 CART and Random Forests

There are a plethora of supervised classification algorithms that are suitable candidates for the task of estimating the expected loss. As the optimal design procedure estimates the expected loss many times, we require a fast classification method. As a generic and fast nonparametric classification approach, we adopt classification and regression trees (CART, see Breiman et al. (1984)) to estimate the expected loss at each design visited during the design procedure.

The CART algorithm generates a binary tree where each internal node consists of one binary rule that involves exactly one of the features, e.g., $y_3 < 10$. The feature space is split recursively at the internal nodes according to the binary rules, thereby creating a partition of the feature space consisting of hyperrectangles aligned along the feature axes. Each terminal node or leaf contains all the observations in the training sample which fall into the associated hyperrectangle. The hyperrectangle region of the feature space associated to a leaf is defined by the binary rules in the nodes leading to that leaf. For a classification tree, the class label which is assigned to a particular region of the feature space is determined by majority vote of the training samples in the corresponding leaf. The class proportions of the training samples in a leaf can be used to obtain crude estimates of the posterior class probabilities for observations falling into the associated feature space region.

Trees are constructed recursively beginning at the root. Each leaf contains those training samples that meet all the conditions leading down the path from the root to that leaf. If no stopping criterion is met and the leaf's sample contains more than one distinctive feature

value, the leaf is split into two daughter nodes and becomes an internal node. To that end, the binary rule that splits the sample at the node into two subsets for the two new leaves has to be determined. The feature variable and the split point are selected such that a given criterion is minimised across all subsets. For classification, the default criterion of node impurity used for growing the tree is the Gini index $\sum_{m=1}^K \hat{p}_m(1 - \hat{p}_m)$, where \hat{p}_m is the proportion of training samples from class m in the node.

As noted for example by Hastie et al. (2009), fully grown trees, where no further splits are possible, usually overfit the data. Therefore, one might stop earlier and define a minimum size of a node or a parent node. More preferably, one can grow a full tree and prune it afterwards according to a cost-complexity criterion that incorporates the node impurities and the number of terminal nodes. For an efficient algorithm to find the optimal pruned tree see Breiman et al. (1984). The optimal choice of the minimum node size or the tuning parameters for cost-complexity pruning can be determined by cross-validation.

Exploiting the similarities between trees and nearest neighbour classifiers, Breiman et al. (1984) show that the misclassification error rate of a fully grown tree is bounded above by twice the Bayes error rate, which has been shown for 1-nearest neighbour classification by Cover and Hart (1967). It also follows from Breiman et al. (1984) that the misclassification error rate of a classification tree attains the Bayes error rate as the sample size tends to infinity.

The CART algorithm automatically assumes equal prior class probabilities, even if the training sample is not balanced. This is achieved by dividing the class counts in the leaves by the overall class counts in the training sample. Therefore, a given leaf is classified as

$$\arg \max_{m \in \{1, \dots, K\}} \frac{N_m(\text{leaf})}{N_m(\text{root})}, \quad (3.2)$$

where $N_m(\text{leaf})$ and $N_m(\text{root})$ are the number of observations from class m in the leaf and in the entire training sample, respectively. One may switch off this mechanism if the training sample reflects the true prior class probabilities. It is also possible to provide user-defined prior class probabilities. In that case the fractions in (3.2) are multiplied by these user-defined prior probabilities.

One disadvantage of trees is their high variance. Slight changes in the data might lead to widely different trees. The reason is the recursive nature of their construction. A suboptimal split at a top node affects the whole tree structure below that node. To reduce the variance, an ensemble method called *bagging* was proposed by Breiman (1996).

Bagging means to draw B bootstrap samples from the training sample and to apply the classification method to each bootstrap sample. As a result, one obtains B different classifiers trained on the B bootstrap samples. The class of a new observation \mathbf{y}_* is predicted by casting a majority vote among the class predictions returned by the B classifiers. Bagging has been shown to be particularly useful for classification methods that are unstable and exhibit a high variance such as trees and neural networks, where bagging can lead to a substantial reduction of the variance.

An ensemble of bagged trees might be highly correlated, which has a negative effect on the variance of the bagged predictor. To reduce the variance further, *random forests* (Breiman, 2001) seek to de-correlate the trees by considering only a random subset of the feature variables

for splitting the tree at each node when the trees are grown. For classification, the default setting is to consider $\lfloor \sqrt{p} \rfloor$ variables at each node, where p is the total number of feature variables. The random selection of feature subsets reduces the correlation between the trees but it also increases the bias of the trees. On the other hand, the trees used in random forests are normally not pruned, and unpruned trees have less bias than pruned trees.

Random forests have been used successfully in many applications and compare favourably to many other more computationally intensive classification methods such as boosting or neural networks, see Hastie et al. (2009). Their nonparametric nature allows for capturing complex dependencies between the model indicator and the features and so they are more flexible than many parametric methods such as logistic regression. Another advantage of trees and random forests is that the scaling of the features does not matter, so there is no need to standardise or transform the features. For our purpose it is also important that random forests do not require any tuning for each new dataset and design because the standard settings work reasonably well in most situations.

Pudlo et al. (2016) note that random forests can easily cope with many noisy, weakly informative and correlated input features. Nevertheless, if the dimension of the raw data is very high, summary statistics may need to be used to improve the classification performance. However, random forests make it possible to include a relatively large amount of informative summary statistics, which alleviates the inaccuracies of using non-sufficient summary statistics for Bayesian model selection reported by Robert et al. (2011). The standard kernel-based ABC approaches for intractable likelihood problems suffer from the curse of dimensionality much more strongly and require low-dimensional summary statistics to work efficiently.

A further advantage of random forests is that no extra test set \mathcal{T}_* is required to estimate the misclassification error rate in Equation (3.1). Each tree is constructed from a bootstrap sample of the training set. The bootstrap samples are drawn from the training set with replacement. It follows that about one third of the training set is omitted in each bootstrap sample. It is therefore possible to make predictions for each training sample \mathbf{y}_i based on those trees where \mathbf{y}_i does not appear. These *out-of-bag* class predictions can then be used to estimate the misclassification error rate. Out-of-bag sampling is qualitatively similar to leave-one-out cross-validation.

Random forests also provide estimates for the posterior model probabilities $p(m|\mathbf{y}, \mathbf{d})$. The estimates are formed by simply averaging the posterior model probability estimates obtained from the trees in the forest. Due to the averaging, the posterior model probability estimates of the random forest are much more stable than those given by a single tree.

Unfortunately, it is not possible to use a separate test sample or out-of-bag samples to estimate the expected multinomial deviance loss given by Equation (2.1) by classification trees or random forests. For a single tree, the lack of smoothness of its posterior model probability estimates means that for an independent test sample the estimated posterior model probability of the true model is almost certainly 0 for at least one observation. That is, $\hat{p}_{MD}(m_*^j|\mathbf{y}_*^j, \mathbf{d}) = 0$ for at least one $j \in \{1, \dots, J_*\}$, and so $-\log[\hat{p}_{MC}(m_*^j|\mathbf{y}_*^j, \mathbf{d})] = \infty$ and the estimate for the expected multinomial deviance loss is also ∞ . When using random forests evaluated on a test sample or via out-of-bag sampling, it is also very likely that some probability estimates are 0. However, evaluating random forests without out-of-bag sampling on the training sample is also not meaningful since the classification accuracy of the full random forest

on the training sample is usually 1. Therefore, we cannot use random forests to estimate the expected multinomial deviance loss. When using classification trees, the multinomial deviance loss has to be estimated imperfectly on the training sample.

3.3 Assessing the Performance of a Design

In our optimal design procedure we have to estimate the expected loss criterion many times. In some cases it may not be feasible to use an accurate but computer-intensive classification method like a random forest or to generate a separate test set for each design. Instead, we may need to employ a quick classification procedure like a tree evaluated on the training set that leads to overfitting. If the ranking of the designs is not affected too strongly by the overfitting, we can still get reasonably efficient designs with this strategy.

Once we have found one or several optimal designs, we are also able to assess the performance of those designs with the classification method. For example, it may be of interest to assess the ability to discriminate between models as the sample size or design dimension is increased. For this assessment to be accurate, it is important that the classifiers do not overfit the data on which they are evaluated, as this might produce misleading results. Given that only a relatively small number of designs need to be assessed, we suggest that more effort can be placed in the classification procedure. For example, we can simulate both a training and a test set. On the training set, we can apply for example a tree with k -fold cross-validation to find a model that performs well on untrained data. Alternatively, we can train a random forest with a large number of trees. Then, the classification performance in terms of the misclassification error rate and the misclassification matrix can all be estimated by applying the fitted model to the test dataset.

The *misclassification* or *confusion matrix* contains for each combination of true model m_i (in the rows) and predicted model m_j (in the columns) the proportions of samples from true model m_i that were classified as model m_j . The misclassification matrix is computed on a separate test set or using out-of-bag samples in the case of random forests. It provides a comprehensive picture of the classification accuracy of a method at a given design.

4 Examples

In this section we consider several examples to highlight the utility of our proposed method. To perform the design optimisation, we use a modification of the coordinate exchange (CE) algorithm (Meyer and Nachtsheim, 1995), which involves cycling through each of the design variables iteratively, trialling a set of candidate replacements and updating the value of the design variable if the objective/loss function is reduced. This is continued until no updates to the design are made in a given cycle. To guard against possible local optima, we run the algorithm in parallel 20 times with random starts. We acknowledge the stochastic nature of our objective function by considering the (up to) six last designs visited in each of the 20 runs as candidates for the overall optimal design. For each of the candidates, we compute the loss function ten times to reduce the noise. The chosen optimal design is the one with the lowest average loss among the candidate designs. A detailed description of the optimisation algorithm that we employ is provided in Appendix A. We do not expend any effort on finding

Model Number	Event Type	Update	Rate
Model 1	Infected	$S(t) - 1, I(t) + 1$	$b_1^{(1)} S(t)$
Model 2	Infected	$S(t) - 1, I(t) + 1$	$[b_1^{(2)} + b_2^{(2)} I(t)] S(t)$
Model 3	Exposed	$S(t) - 1, E(t) + 1$	$b_1^{(3)} S(t)$
	Infected	$E(t) - 1, I(t) + 1$	$\gamma^{(3)} E(t)$
Model 4	Exposed	$S(t) - 1, E(t) + 1$	$[b_1^{(4)} + b_2^{(4)} I(t)] S(t)$
	Infected	$E(t) - 1, I(t) + 1$	$\gamma^{(4)} E(t)$

Table 1: Four competing models considered in the infectious disease example of Section 4.1.

Model Number	Parameter	Prior
Model 1	$b_1^{(1)}$	$\mathcal{LN}(-0.48, 0.15)$
Model 2	$b_1^{(2)}$	$\mathcal{LN}(-1.1, 0.2)$
	$b_2^{(2)}$	$\mathcal{LN}(-4.5, 0.6)$
Model 3	$b_1^{(3)}$	$\mathcal{LN}(-0.54, 0.15)$
	$\gamma^{(3)}$	$\mathcal{E}(0.01)$
Model 4	$b_1^{(4)}$	$\mathcal{LN}(-1.34, 0.41)$
	$b_2^{(4)}$	$\mathcal{LN}(-4.26, 0.25)$
	$\gamma^{(4)}$	$\mathcal{E}(0.01)$

Table 2: The prior distributions considered for the infectious disease example of Section 4.1. Here $\mathcal{LN}(\mu, \sigma)$ denotes the lognormal distribution with location μ and scale σ . $\mathcal{E}(\eta)$ denotes the exponential distribution with rate η .

the best optimisation algorithm for each of the examples as this is not the focus of the paper. We find that the CE algorithm performs adequately to illustrate the findings of the paper.

4.1 Stochastic Models in Epidemiology

An example involving four competing Markov process models for the spread of an infectious disease is considered in Dehideniya et al. (2018). Let $S(t)$, $E(t)$ and $I(t)$ denote the number of susceptible, exposed and infected individuals at time t in a closed population of size $N = 50$ such that $S(t) + E(t) + I(t) = N$ for all t . The possible transitions in an infinitesimal time δ_t for each of the four models are shown in Table 1. Models 1 – 4 are referred to as the death, SI, SEI and SEI2 models, respectively. Models 1 and 2 do not have an exposed population. The algorithm of Gillespie (1977) can be used to efficiently generate samples from all the models. The prior distributions for all the parameters of each model are shown in Table 2. All models are assumed equally likely *a priori*.

We consider the design problem of determining the optimal times (in days) $\mathbf{d} = (d_1, d_2, \dots, d_n)$, where $d_1 < d_2 < \dots < d_n \leq 10$, to observe the stochastic process in order to best discriminate between the four models under the available prior information. Only the $I(t)$ population can be observed. Unfortunately, the likelihood functions for Models 2 – 4 (especially the SEI and SEI2 models) are computationally cumbersome as they require computing the ma-

trix exponential (see, e.g., Drovandi and Pettitt (2008)). Whilst computing a single posterior distribution is feasible, as in a typical data analysis, computing the posterior distribution or posterior model probabilities for thousands of prior predictive datasets, as in a standard optimal Bayesian design approach, is computationally intractable.

Dehideniya et al. (2018) develop a likelihood-free approach based on approximate Bayesian computation (ABC) to solve this model discrimination design problem. Given a particular level of discretisation of the design space (time in this case), the ABC approach involves simulating a large number of prior predictive simulations at all discrete time points and storing them in the so-called reference table. The size of the reference table is manageable in this example because the dimension of the design points is only one (time) and each observation (number of infected individuals at time t) is univariate. Then, for a particular draw from the prior predictive distribution, \mathbf{y} , at some proposed design, \mathbf{d} , the ABC rejection algorithm of Grelaud et al. (2009) is used to estimate the posterior model probabilities and in further consequence the loss functions. The posterior model probability $p(m|\mathbf{y}, \mathbf{d})$ is estimated by computing the proportion of model m simulations in the retained sample, where the retained sample is composed of those simulations from the reference table which are ‘closest’ to the dataset \mathbf{y} . The size of the retained sample is only a very small fraction of the size of the reference table. The reader is referred to Dehideniya et al. (2018) for more details. Price et al. (2016) make use of the discrete nature of the data to efficiently estimate the expected loss. They average the loss over all the unique datasets from the reference table instead of using a separate sample from the prior predictive distribution.

For each of the classification methods, we use a sample of 5K simulations from each model to train the classifier at each new design. For the classification trees, we estimate the expected 0–1 loss at each design by evaluating the classifier either on the training sample or on a separate test sample of the same size as the training sample. As mentioned in Section 3.2, it is not possible to estimate the expected multinomial deviance loss by using random forests or trees evaluated on a test sample. We could follow the ABC method and draw the simulations for the training and test samples from a large bank of prior prediction datasets simulated at the whole design grid to reduce the computing time. However, since the classification method requires significantly fewer simulations, we find that it is still fast to draw a fresh dataset for each proposed design. For the ABC approach, the reference table contains 100K stored prior predictive simulations for each model. To compute the expected loss, we average the estimated loss over 500 draws from $p(\mathbf{y}|m, \mathbf{d})$ for each model and retain a sample of size 2K from the reference table for each draw.

Figure 1 shows the approximate expected loss functions for 1 design observation under several estimation approaches and loss functions: the ABC approach for the 0–1 loss and the multinomial deviance loss, the classification approach using trees evaluated on the training sample for the 0–1 loss and the multinomial deviance loss, the classification approach using trees evaluated on a separate test sample for the 0–1 loss, and the classification approach using random forests for the 0–1 loss. It is evident that all the functions are qualitatively similar and produce the same optimal design around 0.5 – 0.75 days. However, the times needed to construct the curves are vastly different. For the 0–1 loss, it took less than 1 minute for the two tree classification approaches, about 4.3 minutes for the random forest classification approach, and more than 18 minutes using 4 parallel cores for the ABC approach to generate the respective graphs. Despite the much higher simulation effort needed for the ABC approach,

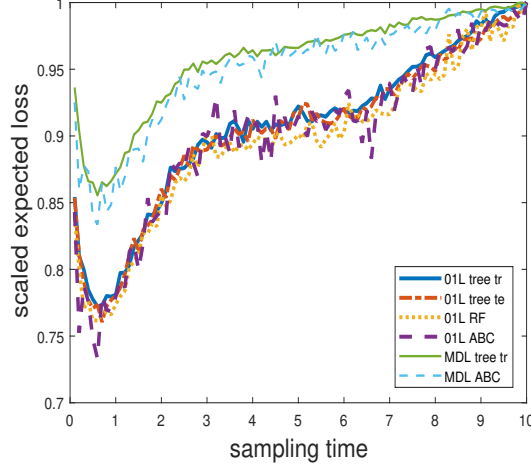


Figure 1: Plots of the approximated expected loss functions produced by the tree classification approach with no test sample (solid), the tree classification approach using a test sample (dash-dotted), the random forest classification approach (dotted), and the ABC approach (dashed) under the 0–1 loss (thick lines) and multinomial deviance loss (thin lines) for the infectious disease example. The expected losses have been scaled by dividing through the maximum loss for an easier comparison.

its estimates of the expected loss functions are still considerably noisier than the estimates of the classification approaches.

The optimal designs obtained by the classification and ABC approaches are shown in Tables 3 and 4. The test set-evaluated tree and the random forest classification approach lead to designs with a general preference for later sampling times. The designs obtained by using trees evaluated on the training set cluster around the early sampling times with no sampling time greater than 4.25. The ABC approach produces designs in between these two extremes. It is interesting to note that the designs vary much more between different loss estimation approaches than they vary between the different loss functions. This reaffirms our decision to consider only the 0–1 loss in the other examples.

Method/Loss	$n = 1$			$n = 2$			$n = 3$		
Tree train 01L	0.75	1.00	3.75	0.75	1.75	3.50	0.75	1.75	3.50
Tree test 01L	0.50	0.75	4.50	0.75	4.25	10.00	0.75	4.25	10.00
RF 01L	0.50	0.75	4.50	0.75	4.00	7.75	0.75	4.00	7.75
ABC 01L	0.50	0.75	4.00	0.25	1.00	4.75	0.25	1.00	4.75
Tree train MDL	0.75	0.75	3.75	0.75	1.50	3.25	0.75	1.50	3.25
ABC MDL	0.50	0.75	4.50	0.50	1.50	4.75	0.50	1.50	4.75
Equidistant	5.00	3.33	6.67	2.50	5.00	7.50	2.50	5.00	7.50

Table 3: Optimal designs obtained by classification (random forest or tree evaluated on the training or test sample) and ABC approaches under the 0–1 loss (01L) or multinomial deviance loss (MDL) ($n = 1, 2$, and 3) for the infectious disease example. The equidistant designs are also shown.

Method/Loss	$n = 4$				$n = 5$				
Tree train 01L	0.50	1.25	2.00	3.75	0.50	1.00	1.50	2.50	4.25
Tree test 01L	0.75	4.25	9.50	10.00	0.75	4.00	9.25	9.75	10.00
RF 01L	0.75	4.00	7.50	8.00	0.75	4.00	7.50	8.75	9.50
ABC 01L	0.25	1.00	3.50	6.00	0.25	0.75	1.50	5.25	7.75
Tree train MDL	0.50	1.25	2.25	4.00	0.50	1.00	1.50	2.25	4.00
ABC MDL	0.25	1.25	3.25	5.00	0.75	1.75	3.50	5.25	8.25
Equidistant	2.00	4.00	6.00	8.00	1.67	3.33	5.00	6.67	8.33

Table 4: Optimal designs obtained by classification (random forest or tree evaluated on the training or test sample) and ABC approaches under the 0–1 loss (01L) or multinomial deviance loss (MDL) ($n = 4$ and 5) for the infectious disease example. The equidistant designs are also shown.

As our next step, we compare the optimal designs found under the different approaches using a random forest classifier. For each of the optimal designs, we train a random forest with 100 trees based on 10K simulations from each model. The misclassification error rates and the misclassification matrices are estimated from a fresh set of 10K simulations from each model. The results for all the optimal designs as well as for the equispaced designs are shown in Table 5. For more than two observations, the designs that clearly perform best are those found under the classification approaches that reduce the effect of overfitting on the estimation of the misclassification error rate. This is no surprise since the misclassification error rates are evaluated using random forests. The ABC optimal designs also generally perform well except for $n = 5$ design times. The optimal designs found using trees evaluated on the training set have significantly worse misclassification error rates than the other methods. We can also observe that the loss function used for optimisation has little effect on the performance of the optimal design. The equispaced designs perform substantially worse than all the optimal designs up until $n = 3$ observations. For more observations, the designs found using trees evaluated on the training set are only marginally more efficient than the equispaced designs. Table 5 also shows that there is almost no gain in the classification performance by increasing the number of observations beyond 2. Any additional observation will only add a negligible amount of information regarding model discrimination. At some point, adding additional uninformative observations adversely affects the classification power of the random forest.

In this example, the resulting designs of the classification approach differ greatly whether the effect of overfitting on the estimation of the expected loss is taken into account or not. Whenever computationally feasible, we advocate to estimate the expected loss using a test sample so that the expected loss is not constantly underestimated during the design phase. If sampling from the model is cheap, like in the current example, generating a test sample comes at little additional cost. If simulation is more time-intensive, one may consider using random forests, for which the estimated loss can be estimated via out-of-bag sampling without needing a separate test sample.

The results of the random forest classifications at the optimal designs were also used to compute the misclassification matrices for those designs. For the tree classification approach using a test sample, the misclassification matrices for 1 – 4 time points are shown in Figure 2. The figure suggests that it is difficult to discriminate between models 1 and 3 and also models 2 and 4. This is not surprising given that we do not observe the exposed population. The

Design	$n = 1$	$n = 2$	$n = 3$	$n = 4$	$n = 5$
Tree train 01L	0.560	0.525	0.532	0.547	0.547
Tree test 01L	0.559	0.522	0.515	0.511	0.512
RF 01L	0.554	0.515	0.511	0.516	0.516
ABC 01L	0.554	0.512	0.518	0.520	0.540
Tree train MDL	0.560	0.523	0.541	0.542	0.551
ABC MDL	0.557	0.515	0.522	0.529	0.536
Equidistant	0.661	0.617	0.571	0.552	0.551

Table 5: Misclassification error rates for optimal designs obtained by classification (random forest or tree evaluated on the training or test sample) and ABC approaches under the 0–1 loss (01L) or multinomial deviance loss (MDL) as well as for the equidistant designs for the infectious disease example.

misclassification matrices for the other loss estimation approaches and loss functions can be found in the Appendix C. They are qualitatively all very similar to Figure 2.

Finally, we compare the optimal designs based on approximate posterior model probabilities estimated using ABC. To that end, we simulate 50 datasets from each of the 4 models at the optimal designs and estimate the posterior model probability of the true model using ABC rejection. To get precise estimates of the posterior model probabilities for each of the 200 datasets, we generate 10 million simulations from the prior predictive distribution to build the reference table. To estimate the posterior probabilities for each generated dataset, we retain 40K simulations from the reference table. Compared to the ABC sampler used for finding the design, we retain 0.1% instead of 0.5% of the reference table and the reference table is one hundred times larger. By retaining a smaller proportion of a larger reference table, the ABC approximation improves. Boxplots of the estimated model probabilities for all the optimal designs as well as for the equispaced designs for 1 – 5 observations are shown in Figure 3. It can be seen that the results for all the different optimal designs are very similar, even though the approaches using the 0–1 loss criterion do not directly target the improvement of the posterior model probabilities. The equispaced designs perform appreciably worse up until $n = 4$ observations. It is also evident that, given the prior information in this example, not much gain can be achieved by collecting more than two observations, which is similar to the classification results obtained in Table 5. Assessing the optimal designs using random forests is much faster than performing this ABC simulation study.

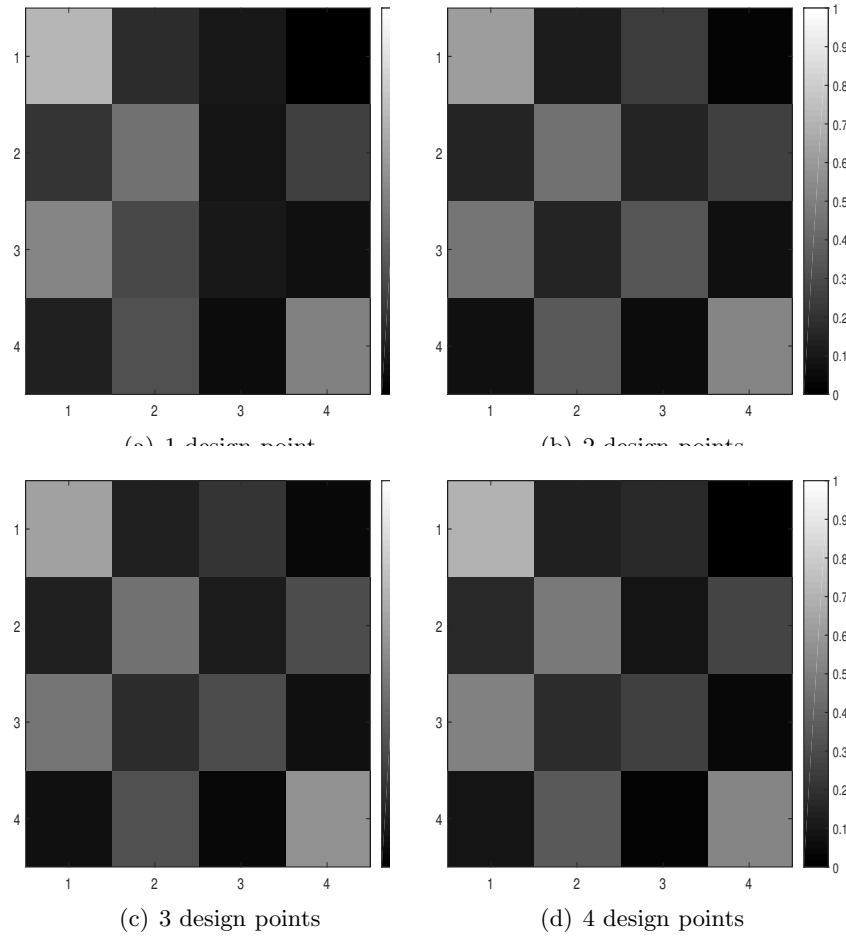


Figure 2: Misclassification matrices obtained for the *tree classification designs (using test samples)* under the $0-1$ loss for the infectious disease example. Designs for 1 – 4 observations are considered.

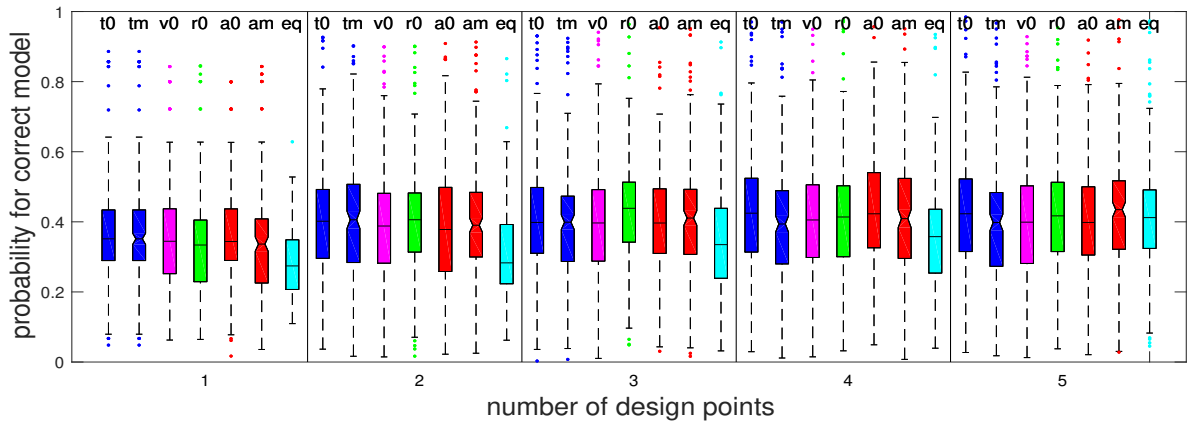


Figure 3: Boxplots of estimated ABC posterior model probabilities of the correct model for 200 simulated datasets (50 from each of the four models) in the infectious disease example. The datasets are simulated at the optimal designs for the different approaches for 1 – 5 observations. For each number of design points, from left to right there are two blue boxplots for the training set-evaluated tree classification designs (t0 and tm), one magenta boxplot for the test set-evaluated tree classification design (v0), one green boxplot for the random forest classification design (r0), two red boxplots for the ABC classification designs (a0 and am), and one cyan boxplot for the equispaced design (eq). Boxplots for the 0–1 loss and for the equispaced designs do not have a notch, whereas boxplots for the multinomial deviance loss are notched.

4.2 Macrophage Model

A common challenge in experimental biology is identifying the unobserved heterogeneity in a system. Consider for example the experimental system in Restif et al. (2012). In this system, the authors wished to identify the role of antibodies in modulating the interaction of intracellular bacteria – in particular, *Salmonella enterica* serovar Typhimurium (*S. Typhimurium*) – with human phagocytes, inside which they can replicate. The experiments assessed the effect of a number of different human immunoglobulin subclasses on the intracellular dynamics of infection by combining observed numbers of bacteria per phagocyte with a mathematical model representing a range of different plausible scenarios. These models were fit to experimental data corresponding to each human immunoglobulin subclass in order to determine the underlying nature of the interactions between the antibodies and bacteria. In these experiments, the data demonstrated bimodal distributions in the number of intracellular bacteria per phagocytic cell. The aim was to identify the source of the unobserved heterogeneity in the system that caused the observed patterns. Specifically, is there underlying heterogeneity in the bacteria’s ability to divide inside phagocytes, or is it the phagocyte population which is heterogeneous in its ability to control bacterial division? In this context, the classification approach allows us to find the experimental design which best enables us to discriminate between these competing hypotheses – (1) unobserved heterogeneity in the bacteria, (2) in the cells, or (3) no heterogeneity.

We give a brief account of the experimental procedure:

- After bacterial opsonisation (i.e., the process by which bacteria are coated by antibodies), the bacteria were exposed to the phagocytic cells for a total of $t_{exp} = 0.75$ hours. During this time, phagocytosis occurred, i.e., the bacteria were internalised by the phagocytic cells.
- Next, the cells were treated with gentomycin, an antibiotic that kills extracellular bacteria, so that phagocytosis stopped.
- At each of the times $t_1 = 1$ and $t_2 = 9$ hours post-exposure, two random samples of $S = 450$ cells were taken from the overall population of cells (i.e., in total $N_{cells} = 1800$): one sample to count the proportion of infected cells (under a low-magnification microscope), and one sample of infected cells to determine the distribution of bacterial counts per infected cell (at higher magnification).

The full experimental procedure is detailed in Restif et al. (2012).

4.2.1 Model

We consider three mathematical models, based on Restif et al. (2012), to represent the three competing hypotheses about heterogeneity. These models are continuous-time Markovian processes that simulate the dynamics of intracellular bacteria within macrophages. Model (1) tracks the joint probability distribution of the number of replicating (R) and non-replicating (D for dormant) bacteria within a single macrophage, assuming all macrophages in a given experiment follow the same distribution. In model (2), each macrophage has a fixed probability q of being refractory, in which case it only contains non-replicating bacteria, and a

probability $1 - q$ of being permissive, in which case it only contains replicating bacteria. In model (3), all macrophages are permissive and all bacteria are replicating.

In all three models, a macrophage can acquire a new bacterium with a constant rate ϕ while there is no antibiotic in the medium ($t < t_{exp}$); this rate then drops to 0 for the remainder of the simulations. In model (1), we assume that a proportion $p > 0$ of available bacteria are non-replicating, so these are acquired by macrophages at rate ϕp , while replicating bacteria are acquired at rate $\phi(1 - p)$. Intracellular bacteria are degraded at rate d for replicating bacteria and rate ϵ for non-replicating bacteria. Within permissive macrophages containing $R > 1$ replicating bacteria, the number of replicating bacteria increases by one every time one of these bacteria divides, but this division rate is assumed to be a decreasing function of R (due to limited resources for bacterial growth within a macrophage), expressed as $a e^{-bR}$, where a is the maximum division rate of bacteria and b is a dimensionless scaling parameter. Finally, in model (1), replicating bacteria within permissive macrophages become non-replicating at rate δ . All these transitions are listed in Table 6.

As with the epidemiological models in our first example, we produce numerical simulations of the three models using the Gillespie algorithm (Gillespie, 1977). In line with the general experimental setup, each macrophage is initially uninfected, but in model (2) it has a probability q of being refractory. This state is set at the start of each simulation and does not change thereafter. To reproduce the data collection process described above, we produce two independent sets of simulations for each observation time t_{obs} in a given experimental design. First, we run S simulations of individual macrophages and record the proportion $\pi(t_{obs})$ of infected macrophages. Second, we run another set of simulations for the same duration until S infected macrophages are obtained, from which we record the proportions $\{\mu_k(t_{obs}), k > 0\}$ of infected macrophages containing k bacteria. This can be repeated multiple times to generate multiple sets of observations from each model m , parameter vector θ_m and experimental design d . Importantly, the simulations' results do not distinguish between replicating and non-replicating bacteria (model 1) or between refractory and permissive macrophages (model 2), as these cannot be told apart by microscopy alone. The aim of the study is to make some inference about the possible heterogeneity among macrophages or bacteria from the models in the absence of direct evidence.

It is possible but cumbersome to compute the likelihood functions for all the models. The number of infected macrophages at time t_{obs} has the binomial distribution $\text{Bin}(S; \mathbb{E}[\pi(t_{obs})])$. Likewise, the vector of numbers of infected macrophages containing $k = 1, \dots, K_+$ bacteria has the multinomial distribution $\text{Mult}(S; \{\mathbb{E}[\mu_1(t_{obs})], \dots, \mathbb{E}[\mu_{K_+}(t_{obs})]\})$. The last category K_+ contains all macrophages with at least K_+ bacteria. The most involved part is to obtain the expected proportions $\mathbb{E}[\pi(t_{obs})]$ and $\mathbb{E}[\mu_1(t_{obs})], \dots, \mathbb{E}[\mu_{K_+}(t_{obs})]$ for any particular set of parameters. A system of linear differential equations for the expected proportions of macrophages that contain a certain number of replicating and non-replicating bacteria can be derived from the continuous-time Markov process models given in Table 6 (see Restif et al. (2012)). This system can be solved using matrix exponentials. However, these operations are quite expensive so that computing the posterior model probabilities becomes very costly. Computing the expected losses and searching for an optimal design can be considered intractable in these circumstances. In contrast, simulations from the models can be obtained very quickly by using the Gillespie algorithm.

Model Number	Event Type	Update	Rate
(1)	Acquisition of R	$R(t) + 1$	$\phi(1 - p)$
	Acquisition of D	$D(t) + 1$	ϕp
	Division	$R(t) + 1$	$a e^{-b R(t)} R(t)$
	Loss of R	$R(t) - 1$	$d R(t)$
	Loss of D	$D(t) - 1$	$\epsilon D(t)$
	Switch of R to D	$R(t) - 1, D(t) + 1$	$\delta R(t)$
(2) Refractory	Acquisition of D	$D(t) + 1$	ϕ
	Loss of D	$D(t) - 1$	$\epsilon D(t)$
(2) Permissive	Acquisition of R	$R(t) + 1$	ϕ
	Loss of R	$R(t) - 1$	$d R(t)$
	Division	$R(t) + 1$	$a e^{-b R(t)} R(t)$
(3)	Acquisition of R	$R(t) + 1$	ϕ
	Loss of R	$R(t) - 1$	$d R(t)$
	Division	$R(t) + 1$	$a e^{-b R(t)} R(t)$

Table 6: Three competing models considered in the macrophage example. $R(t)$ represents the number of replicating bacteria and $D(t)$ the number of non-replicating bacteria within a macrophage. In model (2), a proportion q of macrophages are refractory and $1 - q$ permissive.

The prior distributions used for the three models are discussed in Appendix D.

4.2.2 Design Choices

Recall that in the experiments conducted in Restif et al. (2012), a large number of uninfected cells were exposed to opsonised bacteria for $t_{exp} = 0.75$ hours. After that, $S = 450$ cells were randomly selected at $t_1 = 1$ and $t_2 = 9$ hours to independently assess the proportion of infected cells and the distribution of bacterial counts across infected cells. We note that this is a large number of cells to process in an experiment of this type, and the numbers recorded in similar studies tend to vary greatly (e.g., approximately 20 in Lamberti et al. (2016), 100 in Gorgojo et al. (2014), 500 in Gog et al. (2012)). For the purpose of our example, we consider a realistic scenario where we have the resources to count a fixed number of cells, $N_{cells} = 200$. At each observation time, these cells are equally split between the two independent observational goals, to count the proportion of infected cells and to determine the bacterial count distribution of the infected cells. For example, for an experiment with two observation times this would mean that at each observation time 50 cells are used to establish the proportion of infected cells and 50 different and independently selected infected cells are used to establish the distribution of bacterial counts amongst infected cells. We consider the case where, with this fixed number of cells, we choose the duration of bacteria-phagocyte exposure prior to gentamycin treatment and then select n observation times following gentamycin treatment in order to optimise the classification ability. Our design variables are:

- exposure duration, t_{exp} , which can take the values $\{0.10, 0.20, \dots, 1.50\}$ hours,
- observation times, $\mathbf{t}_{obs} = (t_1, \dots, t_n)$, which can take the values $\{0.25, 0.50, \dots, 10\}$ hours.

That is, a design is composed of $\mathbf{d} = (t_{exp}; \mathbf{t}_{obs})$. In line with the assumption of a constant phagocytosis rate, we select the exposure duration within a short time frame (0 – 1.5 hrs). We consider collecting $n = 1, \dots, 5$ observations for this experiment.

4.2.3 Results

We use the classification approach using classification trees or random forests to determine the optimal designs for discriminating between the three competing models (one model corresponding to each hypothesis) with respect to the misclassification error rate. It is assumed *a priori* that the models are equally likely. We use 5K simulations from the prior predictive distribution of each model during the design process. Tables 7 and 8 show the optimal designs for each classification method and for the different numbers of observation times. The tree and the random forest classification approaches lead to very similar designs.

Similar to the other examples, we assess each design by producing 10K new simulations under each model and using these to train a random forest with 100 trees. A further 10K new simulations per model are then used to estimate the misclassification error rate and the misclassification matrix. The estimated misclassification rates for the designs found under the tree and random forest classification approaches are given in Table 9. For comparison, we also include the estimated error rates for the equispaced designs. The misclassification matrices are given in Appendix E.

Since the optimal designs found using classification trees and random forests are close together, the misclassification error rates between the two approaches are also very similar. The performance of the equispaced designs is clearly worse.

Method	$n = 1$		$n = 2$			$n = 3$			
	t_{exp}	\mathbf{t}_{obs}	t_{exp}	\mathbf{t}_{obs}		t_{exp}	\mathbf{t}_{obs}		
Tree	1.50	10.00	0.30	2.00	10.00	0.30	1.75	9.75	10.00
RF	0.90	10.00	0.10	2.00	10.00	0.10	1.50	10.00	10.00
Equi	0.80	5.00	0.80	3.33	6.67	0.80	2.50	5.00	7.50

Table 7: Optimal classification designs $(t_{exp}; \mathbf{t}_{obs})$ using trees or random forests under the 0–1 loss and equispaced designs for the macrophage model ($n = 1, 2$, and 3).

Method	$n = 4$					$n = 5$				
	t_{exp}	\mathbf{t}_{obs}				t_{exp}	\mathbf{t}_{obs}			
Tree	0.20	1.50	2.75	9.75	10.00	0.20	1.00	2.25	8.50	9.75 10.00
RF	0.10	1.50	2.25	9.75	10.00	0.10	1.50	1.50	10.00	10.00 10.00
Equi	0.80	2.00	4.00	6.00	8.00	0.80	1.67	3.33	5.00	6.67 8.33

Table 8: Optimal classification designs $(t_{exp}; \mathbf{t}_{obs})$ using trees or random forests under the 0–1 loss and equispaced designs for the macrophage model ($n = 4$ and 5).

We are also interested in the posterior model probabilities at the different optimal designs. For each optimal design, we simulate 20 datasets under the prior predictive distribution of each model. For each dataset, we approximate the posterior model probability of the model that

Design	$n = 1$	$n = 2$	$n = 3$	$n = 4$	$n = 5$
Tree	0.192	0.137	0.143	0.145	0.151
RF	0.194	0.132	0.140	0.145	0.148
Equi	0.237	0.198	0.192	0.185	0.193

Table 9: Misclassification error rates for the optimal classification designs using trees or random forests and for the equispaced designs for the macrophage model.

generated the dataset using importance sampling (see, e.g., Liu (2001)) with 50K simulations from the importance distribution. In our case, the prior distribution serves as the importance distribution. Figure 4 shows the boxplots of the posterior model probabilities of the correct model for the different optimal designs. The computations required to generate one of these boxplots ranged from 3.5 hours to more than 10 hours using 24 parallel threads. In contrast, it took less than a minute using four parallel threads to obtain any of the misclassification rates in Table 9.

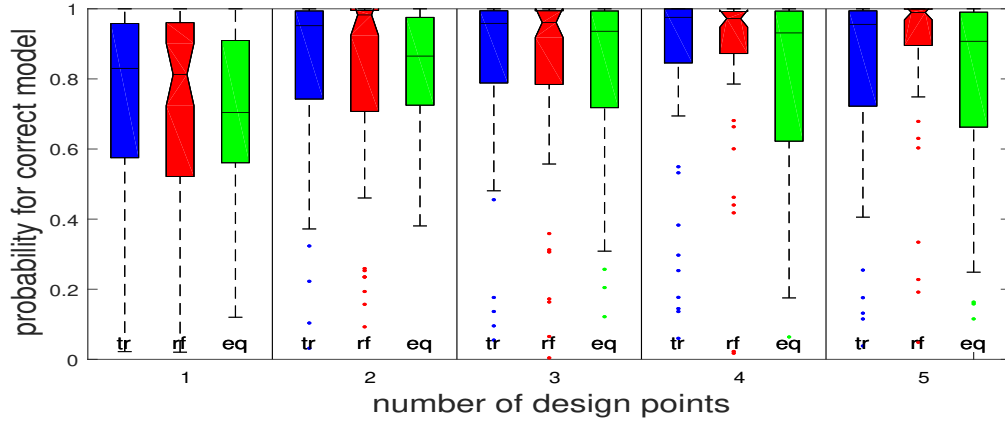


Figure 4: Estimated posterior model probabilities of the correct model for the macrophage example. The results are shown for the optimal classification designs using trees or random forests and for the equispaced designs for 1 – 5 observations. For each number of design points, the blue boxplot on the left-hand side is for the tree classification design (tr), the notched red boxplot in the middle is for the random forest classification design (rf), and the green boxplot on the right-hand side is for the equispaced design (eq).

The number of cells that are able to be counted for the experiment is limited. Given this fixed availability of resources, we can observe a trade-off when the number of observation times increases: more observation times give a better indication of the temporal dynamics of the system but imply a reduced resolution for each additional observation time. The posterior model probabilities in Figure 4 keep improving until three or four observations before starting to decline. Only for the random forest classification designs the posterior model probabilities are highest for $n = 5$ observations. We note that the random forest design for $n = 5$ observations replicates the design point $t = 1.5$ twice and the design point $t = 10$ three times. This suggests a design more akin to two observation times, but where the resources are split 40:60 between the observation times as opposed to a split of 50:50. The distinct observation times stay fairly constant for the random forest designs as the number

of observations increases, only the proportion of cells assigned to the lower or higher design point changes. With respect to the classification power of trees and random forests, Table 9 indicates that two observation times are optimal. For more observations, the higher data dimension impedes the classification accuracy of those methods and more than offsets the gains from having marginally more information in the data due to the more optimal allocation of resources. However, there are no substantial improvements in the posterior probabilities after $n = 2$. Furthermore, especially the random forest classification approach leads to very efficient designs for all design sizes.

Overall, the ability to classify output from the three models and thus to decide between the three competing hypotheses is very good at all the optimal designs. This suggests that we are able to identify with high certainty if heterogeneity is present, and if so, whether the bacteria or the human cells are the source of this heterogeneity.

4.3 Spatial Extremes Example

In this example, the goal is to place a fixed number of measuring sites in space in order to maximise the ability to discriminate between different spatial models for extreme outcomes (e.g., maximum annual temperatures). There are many spatial models for extreme events, see Davison et al. (2012) for an overview. For this example, we consider to discriminate between three isotropic models: two *max-stable* models and one *copula* model.

4.3.1 Models

Max-stable processes are popular for modelling spatial extremes because they are the only possible limits of renormalised pointwise maxima of infinitely many independent copies of a stochastic process (de Haan and Ferreira, 2006). The advantage of working with the limiting process is that no knowledge about the underlying true process is necessary. Inference for extreme outcomes based on the true underlying process is fraught with high uncertainty and most often not feasible because only the tails of the distribution are observed. If the limiting assumption is (approximately) appropriate, it is much easier to model the extreme data according to a max-stable process.

All the univariate marginal distributions of a max-stable process are members of the family of *generalised extreme value (GEV)* distributions. We assume that all the univariate marginal distributions have a *unit Fréchet* distribution ($\Pr\{Y(\mathbf{x}) \leq y\} = \exp\{-1/y\}, y > 0$), so the focus is on modelling the dependence structure of the process. The assumption of unit Fréchet margins is not too restrictive from a practical perspective since a simple transformation can be applied to the univariate margins to make them unit Fréchet distributed, see Davison et al. (2012). The marginal parameters needed for that transformation can be estimated in a separate step. Alternatively, one may estimate the dependence and marginal parameters together.

The *spectral representation* of a max-stable process $\{Y(\mathbf{x}), \mathbf{x} \in \mathcal{X} \subseteq \mathbb{R}^d\}$ with unit Fréchet margins is given by

$$Y(\mathbf{x}) = \max_{i \geq 1} \varphi_i(\mathbf{x}), \quad \mathbf{x} \in \mathcal{X}, \quad (4.1)$$

where the *spectral functions* $\varphi_i(\mathbf{x}) = \zeta_i Z_i(\mathbf{x})$ are the products of the realisations $\{\zeta_i\}_{i=1}^\infty$ of a Poisson point process on the positive real line with intensity $d\Lambda(\zeta) = \zeta^{-2}d\zeta$ and of the independent realisations $\{Z_i(\mathbf{x}), \mathbf{x} \in \mathcal{X}\}_{i=1}^\infty$ of a non-negative stochastic process with continuous sample paths and $E[Z(\mathbf{x})] = 1 \forall \mathbf{x} \in \mathcal{X}$ (see, e.g., Ribatet (2013)).

Different max-stable processes are obtained by choosing different stochastic processes Z . We consider two very popular stationary models, the *extremal- t* model (Opitz, 2013) and the *Brown-Resnick* model with power variogram (Brown and Resnick, 1977; Kabluchko et al., 2009). The specifications for $Z_i(\mathbf{x})$ for each of the models are

$$\begin{aligned} \text{Extremal-}t: \quad & Z_i(\mathbf{x}) = \sqrt{\pi} 2^{-(\nu-2)/2} \Gamma\{(\nu+1)/2\}^{-1} \max\{0, \epsilon_i(\mathbf{x})\}^\nu, \quad \nu > 0, \\ \text{Brown-Resnick:} \quad & Z_i(\mathbf{x}) = \exp\{\varepsilon_i(\mathbf{x}) - \text{Var}[\varepsilon_i(\mathbf{x})]/2\}, \end{aligned}$$

where ϵ_i and ε_i are independent copies of Gaussian processes.

In the case of the extremal- t model, ϵ is a stationary Gaussian process defined by the correlation function $\rho(h)$, where h is the Euclidean distance between two points. For our example, we assume the *powered exponential* or *stable* correlation function:

$$\rho(h) = \exp[-(h/\lambda)^\kappa], \quad \lambda > 0, 0 < \kappa \leq 2. \quad (4.2)$$

The Brown-Resnick process is defined by its semi-variogram. If the process ε is a fractional Brownian motion centred at the origin, the Brown-Resnick process is stationary and the semi-variogram has the form

$$\gamma(h) = (h/\lambda)^\kappa, \quad \lambda > 0, 0 < \kappa \leq 2,$$

where h denotes the distance between two locations.

Both models depend on two parameters governing the dependence between two locations separated by a distance h : the *range* parameter λ and the *smoothness* parameter κ . In addition, the extremal- t model has a *degrees of freedom* parameter denoted by ν . We assume there is no discontinuity of the correlation function at $h = 0$ (i.e., no nugget effect).

The third model we consider is a copula model. Similar to the max-stable models, the univariate marginal distributions of the copula model are unit Fréchet. However, the extremal dependence between the locations is simply modelled by a standard (non-extremal) copula. For an introduction to copulas see Nelsen (2006). We assume the multivariate Student- t copula in our example. The multivariate cumulative distribution function (CDF) at locations $(\mathbf{x}_1, \dots, \mathbf{x}_H)$ implied by the *non-extremal Student- t copula* model (Demarta and McNeil, 2005) is

$$\Pr\{Y(\mathbf{x}_1) \leq y_1, \dots, Y(\mathbf{x}_H) \leq y_H\} = T_{H;\nu}\{T_{1;\nu}^{-1}[F(y_1)], \dots, T_{1;\nu}^{-1}[F(y_H)]; \mathbf{\Sigma}\},$$

where $F(y) = \exp\{-1/y\}$ is the CDF of the unit Fréchet distribution, $T_{1;\nu}^{-1}[\cdot]$ is the quantile function of the univariate Student- t distribution with ν degrees of freedom, and $T_{H;\nu}\{\cdots; \mathbf{\Sigma}\}$

is the CDF of the H -variate Student- t distribution with ν degrees of freedom and dispersion matrix Σ . The diagonal elements of Σ are 1 and the off-diagonal elements contain the correlations between the locations. Therefore, the entries of Σ are given by $\Sigma_{ij} = \rho(h_{ij})$ for $i, j = 1, \dots, H$, where h_{ij} is the distance between locations i and j . As for the extremal- t model, we assume the correlation function to be the powered exponential correlation function (4.2). This also implies that the non-extremal Student- t copula model has the same set of parameters as the extremal- t model: range (λ), smoothness (κ), and degrees of freedom (ν).

4.3.2 Summary Statistics

If a reasonable amount of observations are collected at each location, the data collected quickly becomes very high-dimensional, while each observation is only marginally informative. This diminishes the classification power of the classifiers we use. We therefore aim to reduce the dimension of the data by generating informative summary statistics. Unfortunately, none of the statistics we consider guarantee consistent model choice. This can potentially result in large biases when estimating the posterior model probabilities (Robert et al., 2011), which can also affect the estimates of the misclassification error rates. However, trees and random forests work reasonably well with a sizeable amount of moderately informative feature variables. Therefore, we can include a wide variety of summary statistics, where each contains some information about the process. Considering the combined information of all the summary statistics, we expect that only a small loss in information is incurred compared to the full dataset.

First, we include all the *F-madogram* estimates for all the pairs of locations. The F-madogram (Cooley et al., 2006) is similar to the semi-variogram, but unlike the semi-variogram it also exists if the variances or means of the random variables are not finite. Given n observations $\{y_1(\mathbf{x}_1), \dots, y_n(\mathbf{x}_1)\}$ and $\{y_1(\mathbf{x}_2), \dots, y_n(\mathbf{x}_2)\}$ collected at locations \mathbf{x}_1 as well as \mathbf{x}_2 , the pairwise F-madogram between locations \mathbf{x}_1 and \mathbf{x}_2 is estimated as

$$\hat{\nu}_F(\mathbf{x}_1, \mathbf{x}_2) = \frac{1}{2n} \sum_{i=1}^n |F\{y_i(\mathbf{x}_1)\} - F\{y_i(\mathbf{x}_2)\}|,$$

where $F\{y\} = \exp\{-1/y\}$ is the CDF of the unit Fréchet distribution.

As a second set of summary statistics, we include estimates for all the pairwise *extremal coefficients* (Schlather and Tawn, 2003). For a max-stable process, the pairwise extremal coefficient between locations \mathbf{x}_1 and \mathbf{x}_2 is defined as the value $\theta(\mathbf{x}_1, \mathbf{x}_2)$ for which

$$\Pr(Y(\mathbf{x}_1) \leq y, Y(\mathbf{x}_2) \leq y) = \Pr(Y(\mathbf{x}_1) \leq y)^{\theta(\mathbf{x}_1, \mathbf{x}_2)} = \exp\left(-\frac{\theta(\mathbf{x}_1, \mathbf{x}_2)}{y}\right). \quad (4.3)$$

The pairwise extremal coefficient can assume values between 1 and 2. A value of $\theta(\mathbf{x}_1, \mathbf{x}_2) = 1$ indicates complete dependence between the two locations. If $\theta(\mathbf{x}_1, \mathbf{x}_2) = 2$, the two locations are completely independent. We estimate it using the fast estimator of Coles et al. (1999),

$$\hat{\theta}(\mathbf{x}_1, \mathbf{x}_2) = \frac{n}{\sum_{i=1}^n 1/\max\{y_i(\mathbf{x}_1), y_i(\mathbf{x}_2)\}}. \quad (4.4)$$

The extremal coefficient as defined by (4.3) only exists for max-stable processes. In general, the coefficient also depends on the level y . However, the quantities computed by Equation (4.4) might still provide useful information about the dependence structure. For the t copula model, Lee et al. (2018) demonstrate by simulation that the estimates given by (4.4) are indeed informative about the dependence structure.

The last set of summary statistics we consider is the set of *Kendall's* τ estimates between all pairs of locations. Kendall's τ between locations \mathbf{x}_1 and \mathbf{x}_2 is estimated by

$$\hat{\tau}(\mathbf{x}_1, \mathbf{x}_2) = \frac{2}{n(n-1)} \sum_{1 \leq i < j \leq n} \text{sign}[y_i(\mathbf{x}_1) - y_j(\mathbf{x}_1)] \text{sign}[y_i(\mathbf{x}_2) - y_j(\mathbf{x}_2)].$$

Dombry et al. (2017b) show that for max-stable processes Kendall's τ is equal to the probability that the maxima at two locations occur concurrently and are therefore attained for the same extremal function, so

$$\tau(\mathbf{x}_1, \mathbf{x}_2) = \Pr \left(\arg \max_{i \geq 1} \varphi_i(\mathbf{x}_1) = \arg \max_{i \geq 1} \varphi_i(\mathbf{x}_2) \right).$$

All of the summary statistics we incorporate are also considered by Lee et al. (2018), who perform ABC model selection using the summary statistic projection method of Prangle et al. (2014) for a very similar set of models as in this example. Therefore, a more detailed discussion of the summary statistics can be found in Lee et al. (2018).

4.3.3 Bayesian Inference for Spatial Extremes Models

The likelihood functions of max-stable models are practically intractable for most models for dimensions greater than two or three. Composite likelihood methods have been the most popular way to conduct classical inference for max-stable models, so model discrimination is usually based on the composite likelihood information criterion (CLIC) (Padoan et al., 2010).

The observed extrema at several locations might occur at the same time, which means that the extrema at these locations arise from the same extremal function $\varphi_i(\mathbf{x})$ in Equation (4.1). The locations can then be partitioned according to which extremal functions $\varphi_i(\mathbf{x})$ produce the extreme observations at the different locations. Stephenson and Tawn (2005) show that the joint likelihood of the extreme observations and the partitions is substantially simpler than the likelihood of the extreme observations without knowledge of the partitions. Thibaud et al. (2016) and Dombry et al. (2017a) use this property to devise a Gibbs sampler with the partitions as auxiliary variables to conduct Bayesian inference for max-stable models. However, even the augmented likelihoods are expensive to evaluate for the Brown-Resnick and extremal- t model because they include multivariate Gaussian (Brown-Resnick) and Student- t (extremal- t) CDFs.

Due to the intractability of the likelihoods, ABC has also been a popular method for Bayesian inference of max-stable models, see, e.g., Erhardt and Smith (2012) or the overview in Erhardt and Sisson (2015). Lee et al. (2018) present an ABC application with the joint goal of model selection and parameter estimation for the same set of models we consider. Hainy et al. (2016) seek to find optimal designs for parameter estimation for the extremal- t model with

$\nu = 1$ (called the ‘Schlather model’). They use ABC to estimate the posterior variances, which they use as design criterion. Their design algorithm is confined to very low-dimensional design spaces in order to be able to store the reference table for all possible designs. They sequentially select the best single location among a small set of possible locations. With our classification approach, we are able to overcome these limitations.

4.3.4 Settings and Results

In our example, we want to select H ($H = 3, \dots, 8$) locations on a regular grid such that the ability to discriminate between the three models as measured by the misclassification error rate is optimised. We search the H optimal design points over a regular 6×6 grid laid over a square with edge length 10. The data consist of $n = 10$ independent realisations of the process collected at all the locations. Due to the isotropic nature of the processes, there are potentially many equivalent optimal solutions. With our modified coordinate exchange algorithm using 20 random starts, we seek to find one of these designs or at least a nearly optimal design.

We assume the following prior distributions:

$$\begin{aligned}\log(\lambda) &\sim \mathcal{N}(1, 4), \\ \kappa &\sim \mathcal{U}(0, 2), \\ \log(\nu) &\sim \mathcal{N}(0, 1) \text{ truncated on } [-2.5, 2.5].\end{aligned}$$

Furthermore, we assume equal prior model probabilities ($= 1/3$) for all models.

Simulating from the t copula model is straightforward. It only requires simulating from a multivariate t distribution and then transforming the margins with respect to the univariate t CDF followed by the inverse unit Fréchet CDF. For simulating from the max-stable models, we use the exact simulation algorithm via extremal functions of Dombry et al. (2016).

During the design phase, we use classification trees evaluated on the training set as well as random forests with 500 trees to estimate the misclassification error rates. The training sets for both methods contain 5K simulations per model. The optimal designs obtained for these two methods are provided in Appendix F.

To evaluate the designs found by our classification approach, we repeat estimating the misclassification error rate using random forests with 500 trees on 100 different training sets of size 15K (5K simulations per model). The distributions of the estimated misclassification error rates are plotted in Figure 5. We also include the distributions of the estimated misclassification error rates for 100 training sets generated on 100 randomly selected designs. The optimal classification designs found using random forests clearly perform best for all design sizes. Using classification trees evaluated on the training set instead of random forests leads to designs which are clearly worse (except for $H = 7$). Therefore, not considering the underestimation of the misclassification error rate due to overfitting results in suboptimal designs with respect to the misclassification error rate of the random forest classifier. However, the average misclassification error rate of the classification tree designs is still smaller than the average error rate of the random designs up until 7 design points.

In addition to the misclassification error rate, we also compute the misclassification matrix

yielded by the random forest classifier for each of the 100 training sets for each evaluated design. The average misclassification matrices over the 100 training sets are given in Appendix G for the optimal designs of both methods. They show that discriminating between the two max-stable models is more difficult than discriminating between the t copula model and either of the max-stable models.

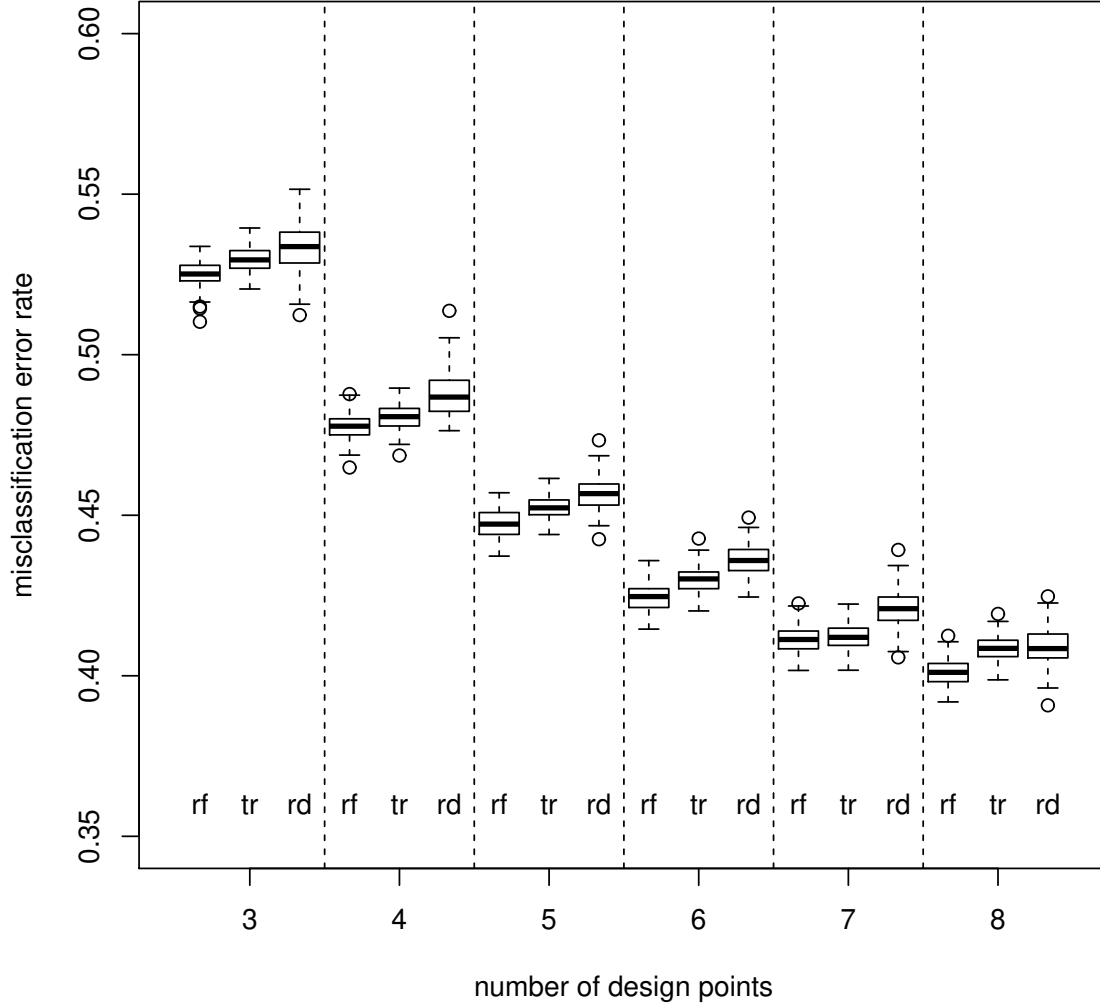


Figure 5: Spatial extremes example: distributions of the random forest-estimated misclassification error rates over 100 random datasets of size 15K generated at the optimal classification designs found using random forests (rf) or trees (tr) for design sizes from three to eight. The distributions of the misclassification error rates over 100 random datasets of size 15K generated at 100 random designs (rd) are also shown for the same design sizes.

5 Discussion

We introduce a new simulation-based Bayesian experimental design approach for model discrimination where the expected loss is estimated via a supervised classification procedure. This approach requires significantly less simulations than other simulation-based approaches based on ABC. Furthermore, efficient, flexible and fast classification methods such as classification trees or random forests can cope with medium to high data dimensions without imposing strict structural assumptions. Therefore, the classification approach significantly increases the scope of design problems which can be tackled compared to previous approaches. For example, optimal designs for the hierarchical logistic regression example could previously only be obtained by assuming normal-based approximations (Overstall et al., 2018a). The high dimensions of the summary statistics for the macrophage and the spatial extremes example render the ABC approach unsuitable or even infeasible. For all the examples we consider the classification approach is significantly more time-efficient than any of the other approaches. The most crucial requirement for the applicability of the classification approach is that efficient samplers are available for all the models.

The methodology we present is rather general. We find that classification trees and random forests work very well in conjunction with the 0–1 loss. They are less suitable for loss functions that directly depend on the posterior model probability such as the multinomial deviance loss. However, one may use any other classification method that is quick and leads to accurate predictions for the application at hand. For example, logistic regression provides natural and smooth estimates for the posterior model probabilities, but it is also less flexible due to the linear form of the predictor. Generalised additive models may improve the accuracy of logistic regression at the expense of a higher computing time. Other fast classification methods include linear discriminant analysis and its extensions like mixture and flexible discriminant analysis. If a higher computing time for the classifier is acceptable and a high predictive power is desired, more elaborate methods such as neural networks may be applied. In general, for most applications it will be preferable to use a classification method where the optimal choice of the tuning parameters is insensitive to the selected design or where standard settings are available that work reasonably well in most circumstances. Otherwise the optimal tuning parameters have to be determined for each new design, for example via cross-validation. Apart from choosing different classification methods, one may also consider different loss functions. The choice of the loss function determines the functional form of the penalty for not correctly estimating the true class. Alternatives to the 0–1 loss and multinomial deviance loss include the exponential, logit, and hinge loss functions. For an overview of all the aforementioned methods and loss functions, see Hastie et al. (2009).

One disadvantage of any simulation-based design approach is that the objective function to optimise over is stochastic. Even though the classification approach reduces the stochastic noise compared to ABC, the optimisation algorithm needs to take the noise into account. Our focus in this paper is not on optimisation, so we use a simple coordinate exchange algorithm on a discretised design space. However, our design algorithm may get stuck at suboptimal solutions if the noise is too large. We try to alleviate that problem by using parallel runs with randomly selected initial designs and by reconsidering the last few designs visited in each run, where the noise is reduced at these designs by evaluating the objective function several times. This algorithm leads to plausible optimal designs in our examples. For all our

examples, the efficiencies of the optimal designs follow a reasonable trajectory as the design sizes are increased. Furthermore, the differences between the design approaches are consistent across the design sizes. For high-dimensional designs with a continuous design space and noisy objective functions, the approximate coordinate exchange algorithm (Overstall and Woods, 2017; Overstall et al., 2018b) is a theoretically sound and efficient alternative. Price et al. (2018) present an ‘induced natural selection heuristic’ algorithm that can cope with moderate to high dimensions and noisy objective functions. Other possible optimisation algorithms suited for noisy objective functions in small to moderate dimensions include ‘simultaneous perturbation, stochastic approximation’ (Spall, 1998a,b) and the rather robust Nelder-Mead algorithm (Nelder and Mead, 1965).

For future work, we will consider extending our approach to Bayesian parameter estimation designs.

Acknowledgements

MH was funded by the Austrian Science Fund (FWF): J3959-N32. DJP and OR were supported by research grant BB/M020193/1 from the Biotechnology and Biological Science Research Council (UK). CCD was supported by an Australian Research Council’s Discovery Early Career Researcher Award funding scheme (DE160100741). Computational resources and services used in this work were provided by the HPC and Research Support Group, Queensland University of Technology, Brisbane, Australia.

References

- Atkinson, A. C., Donev, A. N., and Tobias, R. D. (2007). *Optimum experimental designs, with SAS*. Oxford University Press, New York.
- Atkinson, A. C. and Federov, V. V. (1975a). The design of experiments for discriminating between two rival models. *Biometrika*, 62(1):57–70.
- Atkinson, A. C. and Federov, V. V. (1975b). Optimal design: Experiments for discriminating between several models. *Biometrika*, 62(2):289–303.
- Box, G. E. P. and Hill, W. J. (1967). Discrimination among mechanistic models. *Technometrics*, 9(1):57–71.
- Breiman, L. (1996). Bagging predictors. *Machine Learning*, 24(2):123–140.
- Breiman, L. (2001). Random forests. *Machine Learning*, 45(1):5–32.
- Breiman, L., Friedman, J., Olshen, R. A., and Stone, C. J. (1984). *Classification and Regression Trees*. Chapman & Hall/CRC, Boca Raton.
- Brown, B. M. and Resnick, S. T. (1977). Extreme values of independent stochastic processes. *Journal of Applied Probability*, 14(4):732–739.

- Cavagnaro, D. R., Myung, J. I., Pitt, M. A., and Kujala, J. V. (2010). Adaptive design optimization: A mutual information-based approach to model discrimination in cognitive science. *Neural Computation*, 22(4):887–905.
- Chaloner, K. and Verdinelli, I. (1995). Bayesian experimental design: A review. *Statistical Science*, 10(3):273–304.
- Coles, S., Heffernan, J., and Tawn, J. (1999). Dependence measures for extreme value analyses. *Extremes*, 2(4):339–365.
- Cooley, D., Naveau, P., and Poncet, P. (2006). Variograms for spatial max-stable random fields. In Bertail, P., Soulier, P., and Doukhan, P., editors, *Dependence in Probability and Statistics*, pages 373–390. Springer, New York.
- Cover, T. and Hart, P. (1967). Nearest neighbor pattern classification. *IEEE Transactions on Information Theory*, 13(1):21–27.
- Davison, A. C., Padoan, S. A., and Ribatet, M. (2012). Statistical modeling of spatial extremes. *Statistical Science*, 27(2):161–186.
- de Haan, L. and Ferreira, A. F. (2006). *Extreme Value Theory: An Introduction*. Springer, New York.
- Dehideniya, M. B., Drovandi, C. C., and McGree, J. M. (2018). Optimal Bayesian design for discriminating between models with intractable likelihoods in epidemiology. *Computational Statistics & Data Analysis*, 124:277–297.
- Demarta, S. and McNeil, A. J. (2005). The t copula and related copulas. *International Statistical Review*, 73(1):111–129.
- Dette, H. and Titoff, S. (2009). Optimal discrimination designs. *The Annals of Statistics*, 37(4):2056–2082.
- Devroye, L., Györfi, L., and Lugosi, G. (1996). *A Probabilistic Theory of Pattern Recognition*, volume 31 of *Applications of Mathematics*. Springer-Verlag, New York.
- Dombry, C., Engelke, S., and Oesting, M. (2016). Exact simulation of max-stable processes. *Biometrika*, 103(2):303–317.
- Dombry, C., Engelke, S., and Oesting, M. (2017a). Bayesian inference for multivariate extreme value distributions. *Electronic Journal of Statistics*, 11(2):4813–4844.
- Dombry, C., Ribatet, M., and Stoev, S. (2017b). Probabilities of concurrent extremes. *Journal of the American Statistical Association*, available online.
- Drovandi, C. C., McGree, J. M., and Pettitt, A. N. (2014a). A sequential Monte Carlo algorithm to incorporate model uncertainty in Bayesian sequential design. *Journal of Computational and Graphical Statistics*, 23(1):3–24.
- Drovandi, C. C. and Pettitt, A. N. (2008). Multivariate Markov process models for the transmission of Methicillin-resistant *Staphylococcus aureus* in a hospital ward. *Biometrics*, 64(3):851–859.

- Drovandi, C. C. and Pettitt, A. N. (2013). Bayesian experimental design for models with intractable likelihoods. *Biometrics*, 69(4):937–948.
- Drovandi, C. C., Pettitt, A. N., Henderson, R. D., and McCombe, P. A. (2014b). Marginal reversible jump Markov chain Monte Carlo with application to motor unit number estimation. *Computational Statistics & Data Analysis*, 72:128–146.
- Erhardt, R. J. and Sisson, S. A. (2015). Modelling extremes using approximate Bayesian computation. In Dey, D. K. and Yan, J., editors, *Extreme Value Modeling and Risk Analysis: Methods and Applications*, pages 281–306. Chapman and Hall/CRC.
- Erhardt, R. J. and Smith, R. L. (2012). Approximate Bayesian computing for spatial extremes. *Computational Statistics & Data Analysis*, 56(6):1468–1481.
- Friel, N. and Pettitt, A. N. (2008). Marginal likelihood estimation via power posteriors. *Journal of the Royal Statistical Society: Series B (Statistical Methodology)*, 70(3):589–607.
- Friel, N. and Wyse, J. (2012). Estimating the evidence – a review. *Statistica Neerlandica*, 66(3):288–308.
- Gillespie, D. T. (1977). Exact stochastic simulation of coupled chemical reactions. *The Journal of Physical Chemistry*, 81(25):2340–2361.
- Gog, J. R., Murcia, A., Osterman, N., Restif, O., McKinley, T. J., Sheppard, M., Achouri, S., Wei, B., Mastoeni, P., Wood, J. L. N., Maskell, D. J., Cicuta, P., and Bryant, C. E. (2012). Dynamics of *Salmonella* infection of macrophages at the single cell level. *Journal of the Royal Society Interface*, 9(75):2696–2707.
- Gorgojo, J., Harvill, E. T., and Rodríguez, M. E. (2014). *Bordetella parapertussis* survives inside human macrophages in lipid raft-enriched phagosomes. *Infection and Immunity*, 82(12):5175–5184.
- Grelaud, A., Robert, C. P., Marin, J.-M., Rodolphe, F., and Taly, J.-F. (2009). ABC likelihood-free methods for model choice in Gibbs random fields. *Bayesian Analysis*, 4(2):317–335.
- Hainy, M., Müller, W. G., and Wagner, H. (2016). Likelihood-free simulation-based optimal design with an application to spatial extremes. *Stochastic Environmental Research and Risk Assessment*, 30(2):481–492.
- Hastie, T., Tibshirani, R., and Friedman, J. (2009). *The Elements of Statistical Learning*. Springer, New York.
- Kabluchko, Z., Schlather, M., and de Haan, L. (2009). Stationary max-stable fields associated to negative definite functions. *The Annals of Probability*, 37(5):2042–2065.
- Kass, R. E. and Raftery, A. E. (1995). Bayes factors. *Journal of the American Statistical Association*, 90(430):773–795.
- Key, J. T., Pericchi, L. R., and Smith, A. F. M. (1999). Bayesian model choice: What and why? In Bernardo, J. M., Berger, J. O., and Dawid, A. P., editors, *Bayesian Statistics 6*, pages 343–370. Oxford University Press, New York.

- Konishi, S. and Kitagawa, G. (2008). *Information Criteria and Statistical Modeling*. Springer Series in Statistics. Springer-Verlag, New York.
- Lamberti, Y., Cafiero, J. H., Surmann, K., Valdez, H., Holubova, J., Večerek, B., Sebo, P., Schmidt, F., Völker, U., and Rodríguez, M. E. (2016). Proteome analysis of *Bordetella pertussis* isolated from human macrophages. *Journal of Proteomics*, 136:55–67.
- Lee, X. J., Hainy, M., McKeone, J. P., Drovandi, C. C., and Pettitt, A. N. (2018). ABC model selection for spatial extremes models applied to South Australian maximum temperature data. *Computational Statistics & Data Analysis*, 128:128–144.
- Lindley, D. V. (1956). On a measure of the information provided by an experiment. *Annals of Mathematical Statistics*, 27(4):986–1005.
- Liu, J. S. (2001). *Monte Carlo Strategies in Scientific Computing*. Springer, New York.
- Meyer, R. K. and Nachtsheim, C. J. (1995). The coordinate-exchange algorithm for constructing exact optimal experimental designs. *Technometrics*, 37(1):60–69.
- Nelder, J. A. and Mead, R. (1965). A simplex method for function minimization. *The Computer Journal*, 7(4):308–313.
- Nelsen, R. B. (2006). *An Introduction to Copulas*. Springer, New York, 2nd edition.
- Ng, S. H. and Chick, S. E. (2004). Design of follow-up experiments for improving model discrimination and parameter estimation. *Naval Research Logistics*, 51(8):1129–1148.
- Opitz, T. (2013). Extremal t processes: Elliptical domain of attraction and a spectral representation. *Journal of Multivariate Analysis*, 122:409–413.
- Overstall, A. M., McGree, J. M., and Drovandi, C. C. (2018a). An approach for finding fully Bayesian optimal designs using normal-based approximations to loss functions. *Statistics and Computing*, 28(2):343–358.
- Overstall, A. M. and Woods, D. C. (2017). Bayesian design of experiments using approximate coordinate exchange. *Technometrics*, 59(4):458–470.
- Overstall, A. M., Woods, D. C., and Adamou, M. (2018b). *acebayes: Optimal Bayesian Experimental Design using the ACE Algorithm*. R package version 1.5.
- Padoan, S. A., Ribatet, M., and Sisson, S. A. (2010). Likelihood-based inference for max-stable processes. *Journal of the American Statistical Association*, 105(489):263–277.
- Ponce de Leon, A. C. and Atkinson, A. C. (1992). The design of experiments to discriminate between two rival generalized linear models. In Fahrmeir, L., Francis, B., Gilchrist, R., and Tutz, G., editors, *Advances in GLIM and Statistical Modelling*, volume 78 of *Lecture Notes in Statistics*, pages 159–164. Springer, New York.
- Prangle, D., Fearnhead, P., Cox, M. P., Biggs, P. J., and French, N. P. (2014). Semi-automatic selection of summary statistics for ABC model choice. *Statistical Applications in Genetics and Molecular Biology*, 13(1):67–82.

- Price, D. J., Bean, N. G., Ross, J. V., and Tuke, J. (2016). On the efficient determination of optimal Bayesian experimental designs using ABC: A case study in optimal observation of epidemics. *Journal of Statistical Planning and Inference*, 172:1–15.
- Price, D. J., Bean, N. G., Ross, J. V., and Tuke, J. (2018). An induced natural selection heuristic for finding optimal Bayesian experimental designs. *Computational Statistics & Data Analysis*, 126:112–124.
- Pudlo, P., Marin, J.-M., Estoup, A., Cornuet, J.-M., Gautier, M., and Robert, C. P. (2016). Reliable ABC model choice via random forests. *Bioinformatics*, 32(6).
- Restif, O., Goh, Y. S., Palayret, M., Grant, A. J., McKinley, T. J., Clark, M. R., and Mastoeni, P. (2012). Quantification of the effects of antibodies on the extra- and intracellular dynamics of *Salmonella enterica*. *Journal of the Royal Society Interface*, 10(79).
- Ribatet, M. (2013). Spatial extremes: max-stable processes at work. *Journal de la Société Française de Statistique*, 154(2):156–177.
- Robert, C. P., Cornuet, J.-M., Marin, J.-M., and Pillai, N. S. (2011). Lack of confidence in approximate Bayesian computation model choice. *Proceedings of the National Academy of Sciences of the USA*, 108(37):15112–15117.
- Rose, A. D. (2008). *Bayesian Experimental Design for Model Discrimination*. PhD thesis, University of Southampton.
- Ryan, E. G., Drovandi, C. C., McGree, J. M., and Pettitt, A. N. (2016). A review of modern computational algorithms for Bayesian optimal design. *International Statistical Review*, 84(1):128–154.
- Ryan, E. G., Drovandi, C. C., and Pettitt, A. N. (2015). Simulation-based fully Bayesian experimental design for mixed effects models. *Computational Statistics & Data Analysis*, 92:26–39.
- Ryan, E. G., Drovandi, C. C., Thompson, M. H., and Pettitt, A. N. (2014). Towards Bayesian experimental design for nonlinear models that require a large number of sampling times. *Computational Statistics & Data Analysis*, 70:45–60.
- Schlather, M. and Tawn, J. A. (2003). A dependence measure for multivariate and spatial extreme values: properties and inference. *Biometrika*, 90(1):139–156.
- Scott, J. G. and Berger, J. O. (2010). Bayes and empirical-Bayes multiplicity adjustment in the variable-selection problem. *The Annals of Statistics*, 38(5):2587–2619.
- Spall, J. C. (1998a). Implementation of the simultaneous perturbation algorithm for stochastic optimization. *IEEE Transactions on Aerospace and Electronic Systems*, 34(3):817–823.
- Spall, J. C. (1998b). An overview of the simultaneous perturbation method for efficient optimization. *Johns Hopkins APL Technical Digest*, 19(4):482–492.
- Spiegelhalter, D. J., Best, N. G., Carlin, B. P., and Van Der Linde, A. (2002). Bayesian measures of model complexity and fit. *Journal of the Royal Statistical Society: Series B (Statistical Methodology)*, 64(4):583–639.

- Stephenson, A. and Tawn, J. (2005). Exploiting occurrence times in likelihood inference for componentwise maxima. *Biometrika*, 92(1):213–227.
- Thibaud, E., Aalto, J., Cooley, D. S., Davison, A. C., and Heikkinen, J. (2016). Bayesian inference for the Brown-Resnick process, with an application to extreme low temperatures. *The Annals of Applied Statistics*, 10(4):2303–2324.
- Vajjah, P. and Duffull, S. B. (2012). A generalisation of T-optimality for discriminating between competing models with an application to pharmacokinetic studies. *Pharmaceutical Statistics*, 11(6):503–510.

Appendix A Modified Coordinate Exchange Algorithm

Algorithm 1: Modified coordinate exchange algorithm

Input: Set of available design points \mathcal{A} ; initial design $\mathbf{d} = \{d_1, \dots, d_n\}$ consisting of $n = \text{card}(\mathbf{d})$ design points; function `estimate_loss(\mathbf{d})` that estimates the expected loss for a given design \mathbf{d} ; numbers p and q : for the last (at most) p designs visited the expected loss is estimated q times.

Output: Optimal design $\mathbf{d}^* = \{d_1^*, \dots, d_n^*\}$; average estimated expected loss over q repetitions at \mathbf{d}^* .

```

1 swaps = true;
2 loss = estimate_loss(d);
3 No designs visited so far:  $\mathcal{V} = \{\}$ ;
4 while swaps do
5     swaps = false;
6     for  $i = 1$  to  $n$  do
7         Determine the set of candidate design points  $\mathcal{C} \subseteq \mathcal{A}$ ;
8          $m = \text{card}(\mathcal{C})$ ;
9         Clear lossvec;
10        for  $j = 1$  to  $m$  do
11             $\mathbf{d}^{\text{try}} = \mathbf{d}$ ;
12            Replace element  $i$  of  $\mathbf{d}^{\text{try}}$  with element  $j$  of  $\mathcal{C}$ ;
13            lossvec[ $j$ ] = estimate_loss( $\mathbf{d}^{\text{try}}$ );
14        end for
15        Let minloss = min(lossvec) and  $k$  be the index for which lossvec[ $k$ ] is equal
            to minloss;
16        if minloss < loss then
17            Replace element  $i$  of  $\mathbf{d}$  with element  $k$  of  $\mathcal{C}$ ;
18            loss = minloss;
19            swaps = true;
20            Add  $\mathbf{d}$  to  $\mathcal{V}$ , the history of designs visited so far;
21        end if
22    end for
23 end while
24 Let  $h = \text{card}(\mathcal{V})$  be the number of designs visited, where  $\mathcal{V} = \{\mathbf{d}_1, \dots, \mathbf{d}_h\}$ ;
25 Let  $r = \min(h, p)$ ;
26 for  $i = 1$  to  $r$  do
27     Clear lossvec;
28     for  $j = 1$  to  $q$  do
29         lossvec[ $j$ ] = estimate_loss( $\mathbf{d}_{h-i+1}$ );
30     end for
31     average_lossvec[ $i$ ] = mean(lossvec);
32 end for
33 Let min_average_loss = min(average_lossvec) and  $s$  be the index for which
    average_lossvec[ $s$ ] is equal to min_average_loss;
34 Return  $\mathbf{d}^* = \mathbf{d}_{h-s+1}$  and min_average_loss;

```

In all our examples we set $p = 6$ and $q = 10$.

This algorithm can be run in parallel for different initial designs \mathbf{d} to account for multimodality and local optima. The optimal design selected is the design \mathbf{d}^* returned from the run with the lowest return value for `min_average_loss`. We conduct 20 parallel runs in all our examples.

The selection of the candidate design points in Line 7 depends on the example. For the logistic regression and the macrophage example, there is no restriction and $\mathcal{C} = \mathcal{A}$. For the other examples, the current design points d_1, \dots, d_n in \mathbf{d} have to be excluded since each design point can only be selected once. Furthermore, for the spatial extremes example we only consider design points with the same x- or y-coordinate as the current design point.

Appendix B Logistic Regression Example

We consider the logistic regression example of Overstall and Woods (2017) and Overstall et al. (2018a). The response is binary, $y_{ij} \sim \mathcal{B}(p_{ij})$, and

$$\text{logit}(p_{ij}) = \beta_0 + \gamma_{0i} + \sum_{a=1}^4 v_a (\beta_a + \gamma_{ai}) x_{aij},$$

where $j = 1, \dots, n_G$ and $i = 1, \dots, G$. Here G is the total number of groups and n_G is the number of observations per group. The total number of observations is $n = G \times n_G$. The model parameter of interest is $\boldsymbol{\theta} = (\beta_0, \beta_1, \beta_2, \beta_3, \beta_4)^\top$. The random effect for the i th group is $\boldsymbol{\gamma}_i = (\gamma_{0i}, \gamma_{1i}, \gamma_{2i}, \gamma_{3i}, \gamma_{4i})^\top$. The observed vector of responses for the i th group is $\mathbf{y}_i = (y_{i1}, \dots, y_{in_G})$ and the total dataset is denoted $\mathbf{y} = (\mathbf{y}_1, \dots, \mathbf{y}_G)^\top$. The design vector is the concatenation of the controllable elements of the design matrix, $\mathbf{d} = \{x_{aij}; a = 1, \dots, 4, i = 1, \dots, G, j = 1, \dots, n_G\}$ and is of length $n \times 4$. Each design element is restricted, $x_{aij} \in [-1, 1]$. The variable v_a is an indicator variable that is equal to 1 if the a th predictor is present in the model. It may not be clear which of the four predictors should be included in the model, so there are $2^4 = 16$ possible models to choose from. We aim to select the design \mathbf{d} that maximises our ability to discriminate between all possible models under various prior assumptions as described below.

As in Overstall et al. (2018a), two different model structures are considered. The first structure is that all random effects (RE) are set to 0, resulting in the fixed effects (FE) structure. The second structure is that the random effects are allocated a distribution (RE structure). Within each chosen structure, there are 16 models to discriminate between. In both the FE and RE structures, we use the priors $\beta_0 \sim \mathcal{U}(-3, 3)$, $\beta_1 \sim \mathcal{U}(4, 10)$, $\beta_2 \sim \mathcal{U}(5, 11)$, $\beta_3 \sim \mathcal{U}(-6, 0)$, $\beta_4 \sim \mathcal{U}(-2.5, 3.5)$. We assume that all parameters are independent *a priori*. For the RE model we set $\gamma_{ai} \sim \mathcal{U}(-\zeta_a, \zeta_a)$ and allocate a triangular prior to ζ_a , $p(\zeta_a) = 2(U_a - \zeta_a)/U_a^2$, $0 < \zeta_a < U_a$, where $(U_0, U_1, U_2, U_3, U_4) = (3, 3, 3, 1, 1)$. One possibility for the prior distribution placed on each model is a prior which depends on the number of predictors present in the model. Let (v_{m1}, \dots, v_{m4}) denote the values of (v_1, \dots, v_4) for model m . A model prior accounting for Bayesian multiplicity (Scott and Berger, 2010) is

$$p(m) = \frac{1}{5 \binom{4}{\sum_{a=1}^4 v_{ma}}}. \quad (\text{B.1})$$

In order to estimate the misclassification error rate under the Bayes classifier (the Bayes error rate) for some design \mathbf{d} , we need to estimate posterior model probabilities for J datasets simulated from the prior predictive distribution for each of the models. A common approach for rapid approximation of the evidence for model m , $p(\mathbf{y}|m, \mathbf{d})$, in the context of Bayesian optimal design is importance sampling (IS), where the importance distribution is the prior (e.g. Ryan et al. (2014)). However, if the data is informative (as might be the case in this example if n is large), the number of IS samples to estimate the evidence with reasonable precision may be prohibitively large. The situation is significantly worse for the RE structure, as an importance distribution is required over the space of both the parameter of interest and the random effects (see, e.g., Ryan et al. (2015)). For the FE structure and $n = 48$, using 100K importance samples from the prior and $J = 50$, the time taken to approximate the misclassification error rate for a random design on a cluster using eight parallel threads was almost six minutes. This is very computationally intensive considering that we need to optimise over 48×4 design variables. Performing IS for the RE structure might be considered as completely intractable. Overstall et al. (2018a) propose the use of normal-based approximations to the posterior in the Bayesian design context to provide a convenient estimate of the evidence. They consider the same logistic regression example but use normal priors to facilitate the approximation of the evidence. In some applications, a normal-based approximation may not be adequate.

In contrast, our classification approach avoids computing posterior quantities and requires only simulation from all the models. Interestingly, moving to the RE structure poses little additional difficulty for the classification approach as it remains trivial to simulate from the models. This is a significant advantage of the classification approach.

For the FE structure we consider $n \in \{6, 12, 24, 48\}$ and for the RE structure we consider $n_G = 6$ and $G \in 2, 4, 8$ (to give $n \in \{12, 24, 48\}$). Two prior distributions on the model indicator are trialled: (1) the prior where models are equally likely *a priori* and (2) the prior in (B.1) that corrects for Bayesian multiplicity. We refer to the first as the equal prior and the second as the unequal prior. For this example, the only design criterion that we consider is the misclassification error rate (the expected 0–1 loss). During the design optimisation phase, we estimate the expected loss by classifying the samples of a test sample using a classification tree trained on a separate training sample. The training sample consists of 5K simulations per model, so the total size of the training sample is $16 \times 5K = 80K$. If the prior model probabilities differ from the model proportions in the training sample, the tree-building procedure takes this into account. For the test sample, the model indicators are generated according to the prior model probabilities. We consider a discretised design space for each x_{aij} consisting of the five values $\{-1, -0.5, 0, 0.5, 1\}$.

After having obtained the optimal designs for the different scenarios regarding model structure (FE or RE) and prior distributions (equal or unequal), we attempt to assess the classification performance of these optimal designs using random forests. For each optimal design, 10K simulations under each model are used to train a random forest with 100 trees. A fresh set of $16 \times 10K = 160K$ simulations is used to estimate the misclassification error rate and the misclassification matrix. The model proportions of this test sample reflect the prior model probabilities. The results for the optimal designs of the different scenarios are shown in the rows with bold row labels in Table 10. For each scenario, results for optimal designs under different scenarios as well as a randomly generated design are also provided. For the randomly generated designs, each design point x_{aij} equals 1 or -1 with equal probability.

The results suggest that the optimal designs found for this example are remarkably robust with respect to the assumed model structure (FE or RE) and the assumed prior model probabilities (equal or unequal). The random design has the worst performance under all scenarios. We can also see a decrease in the misclassification error rate as the sample size is increased, as expected.

It is also of interest to see how well the optimal designs found under the tree classification approach perform in terms of posterior model probabilities. We conduct a simulation study under the FE structure using either the equal or the unequal prior. For each design we want to assess, we simulate 800 datasets from the joint distribution $p(\mathbf{y}, m | \mathbf{d})$. For each of the 800 datasets, we approximate the posterior model probability of the model m that generates the dataset \mathbf{y} using IS with 100K prior simulations. As for the classification results in Table 10, we are also interested in the performance of optimal designs found under some wrongly assumed scenarios. We also consider a ‘random’ setup where we select designs randomly for each of the 800 datasets. Figure 6 shows the boxplots of the estimated posterior model probabilities of the correct model for some of the designs of interest when the true scenario is the FE structure with the equal prior. The resulting boxplots when the true scenario is the FE structure with the unequal prior are shown in Figure 7. It is again evident that the optimal designs found are robust under the choice of the structure (FE or RE) and the choice of the prior model probabilities (equal or unequal). We do not perform a simulation study under the RE structure given the increasing difficulty of estimating the posterior model probabilities under this structure.

It is important to note that the random forest-based validation results in Table 10 were obtained in a small fraction of the time that it took to conduct the simulation study used to produce the results in Figures 6 and 7.

Figures 8 – 11 show misclassification matrices for the logistic regression example. To produce the results, 10K simulations from each model are used to train a random forest with 100 trees. The misclassification matrices are then computed based on a fresh test dataset of size $16 \times 10K = 160K$ with model proportions in the dataset corresponding to the prior model probabilities (under the equal prior, 10K simulations are taken from each model). Figures 8 and 9 show misclassification matrices under the FE structure for the equal and unequal priors, respectively. Figures 10 and 11 show the equivalent results for the RE structure. The improvement in classification accuracy is clear as the sample size is increased, less so when increasing from $n = 24$ to $n = 48$. When the unequal prior is selected, it is evident for small sample sizes that it is easier to classify the models with higher prior probability.

FE structure under the equal prior				
Design	Sample Size (n)			
	6	12	24	48
FE equal	0.617	0.496	0.402	0.355
FE unequal	0.647	0.522	0.424	0.381
RE equal	NA	0.503	0.414	0.359
random	0.723	0.592	0.535	0.457
FE structure under the unequal prior				
Design	Sample Size (n)			
	6	12	24	48
FE equal	0.533	0.422	0.331	0.290
FE unequal	0.479	0.406	0.340	0.303
RE unequal	NA	0.406	0.336	0.311
random	0.566	0.452	0.391	0.351
RE model under the equal prior				
Design	Sample Size (n)			
	6	12	24	48
FE equal	NA	0.506	0.412	0.367
RE equal	NA	0.514	0.425	0.371
RE unequal	NA	0.548	0.434	0.400
random	NA	0.651	0.544	0.456
RE model under the unequal prior				
Design	Sample Size (n)			
	6	12	24	48
FE unequal	NA	0.415	0.346	0.312
RE equal	NA	0.433	0.348	0.302
RE unequal	NA	0.411	0.346	0.314
random	NA	0.508	0.407	0.357

Table 10: Shown are the misclassification error rates obtained at various optimal tree classification designs for the different logistic regression models. Four scenarios for the true model are considered: (1) FE structure under the equal prior, (2) FE structure under the unequal prior, (3) RE model under the equal prior and (4) RE model under the unequal prior. Rows with bold labels contain the results for the optimal designs under each scenario. Also shown, for each scenario, are the results for various designs obtained under different wrong scenarios and the results for a random design. The results suggest that the optimal designs found are robust to the model structure (FE or RE) and to the prior model probabilities (equal or unequal). The random design has the worst performance under all scenarios.

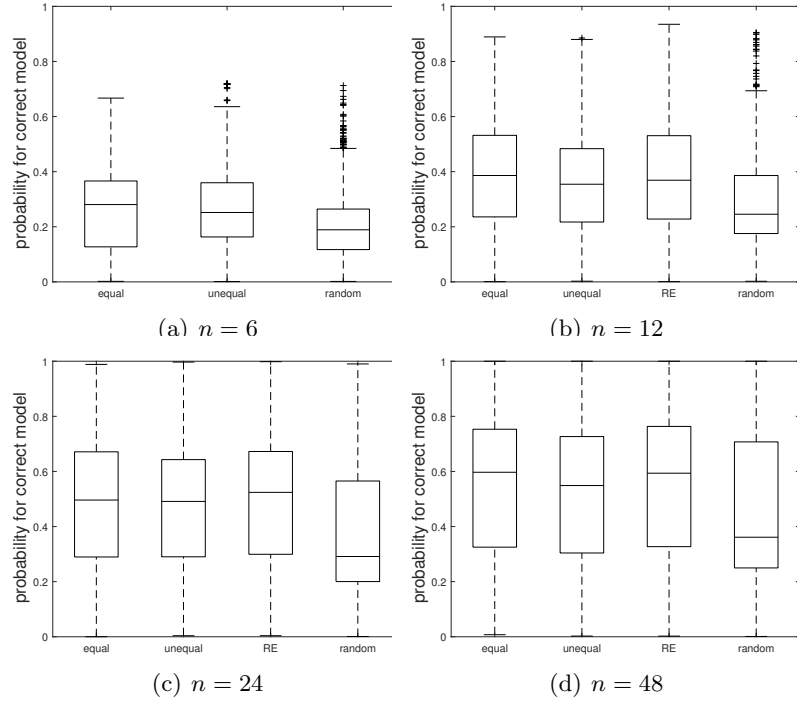


Figure 6: Estimated posterior model probabilities for the correct model by the validation study under the equal prior. Results based on sample sizes of (a) $n = 6$, (b) $n = 12$, (c) $n = 24$ and (d) $n = 48$. Several designs are considered: optimal design found under the correct (equal) prior, optimal design found under the wrong (unequal) prior, optimal design found under the wrong (RE) structure (no results for $n = 6$) and randomly selected designs.

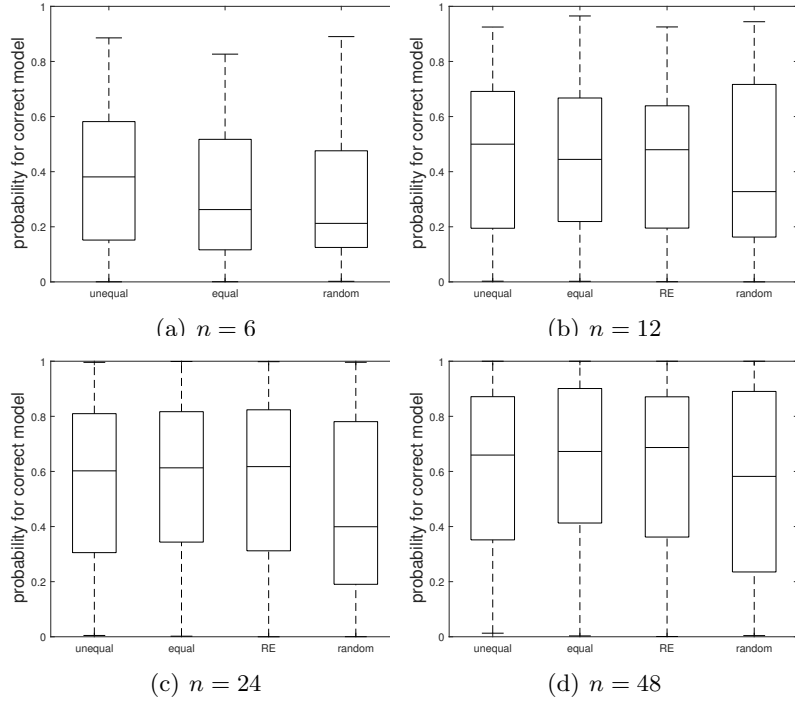


Figure 7: Estimated posterior model probabilities for the correct model by the validation study under the unequal prior. Results based on sample sizes of (a) $n = 6$, (b) $n = 12$, (c) $n = 24$ and (d) $n = 48$. Several designs are considered: optimal design found under the correct (unequal) prior, optimal design found under the wrong (equal) prior, optimal design found under the wrong (RE) structure (no results for $n = 6$) and randomly selected designs.

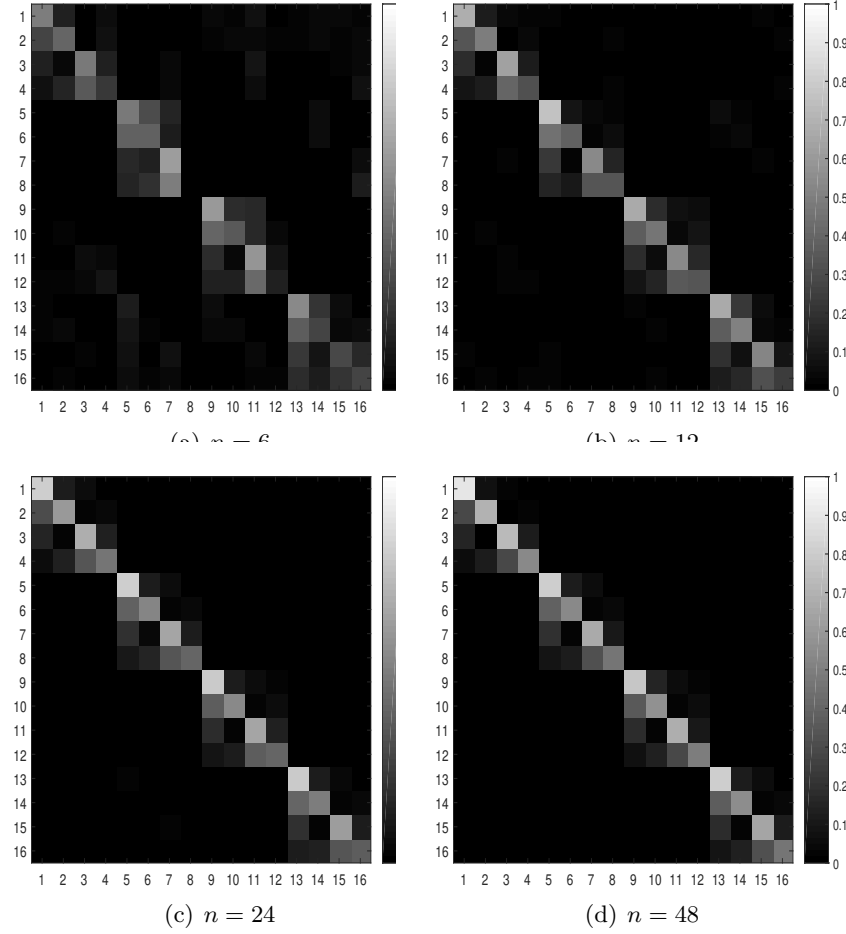


Figure 8: Misclassification matrices obtained for the *FE structures* of the logistic regression example with the *equal prior*.

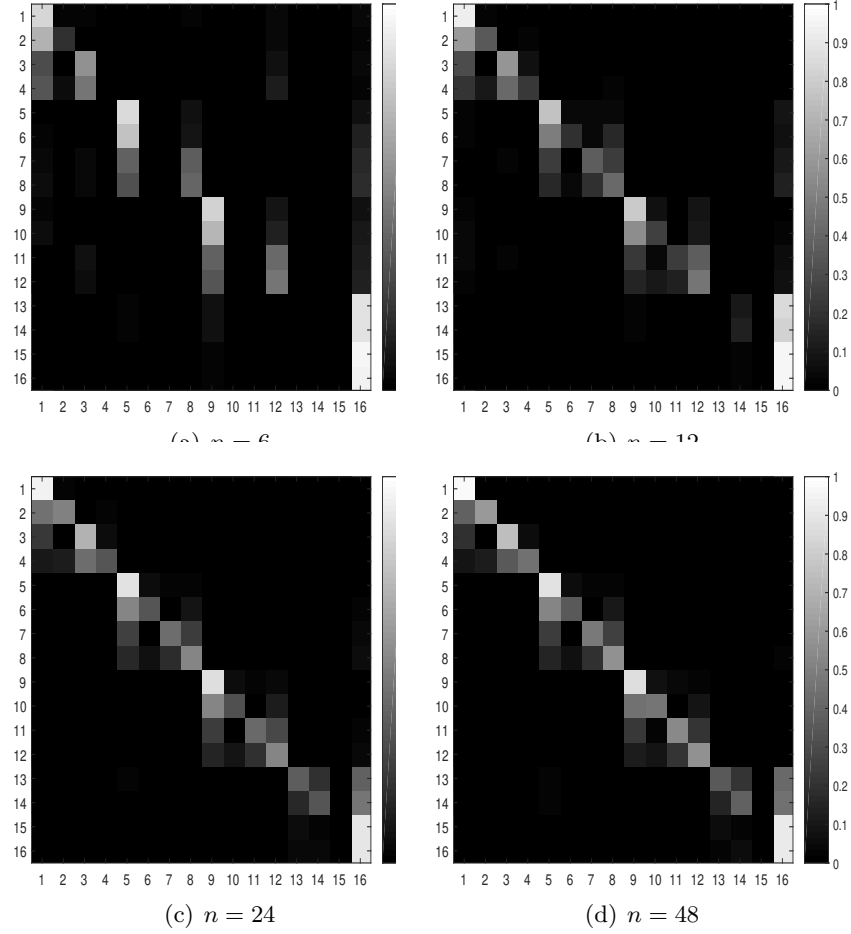


Figure 9: Misclassification matrices obtained for the *FE structures* of the logistic regression example with the *unequal prior*.

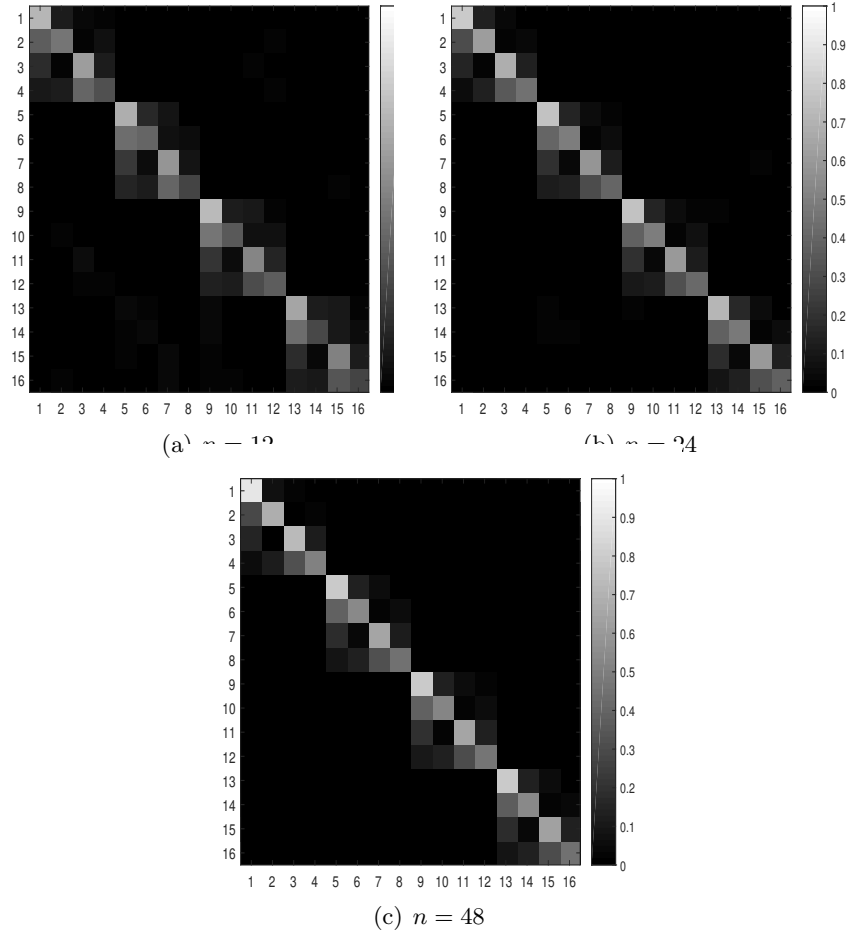


Figure 10: Misclassification matrices obtained for the *RE models* of the logistic regression example with the *equal prior*.

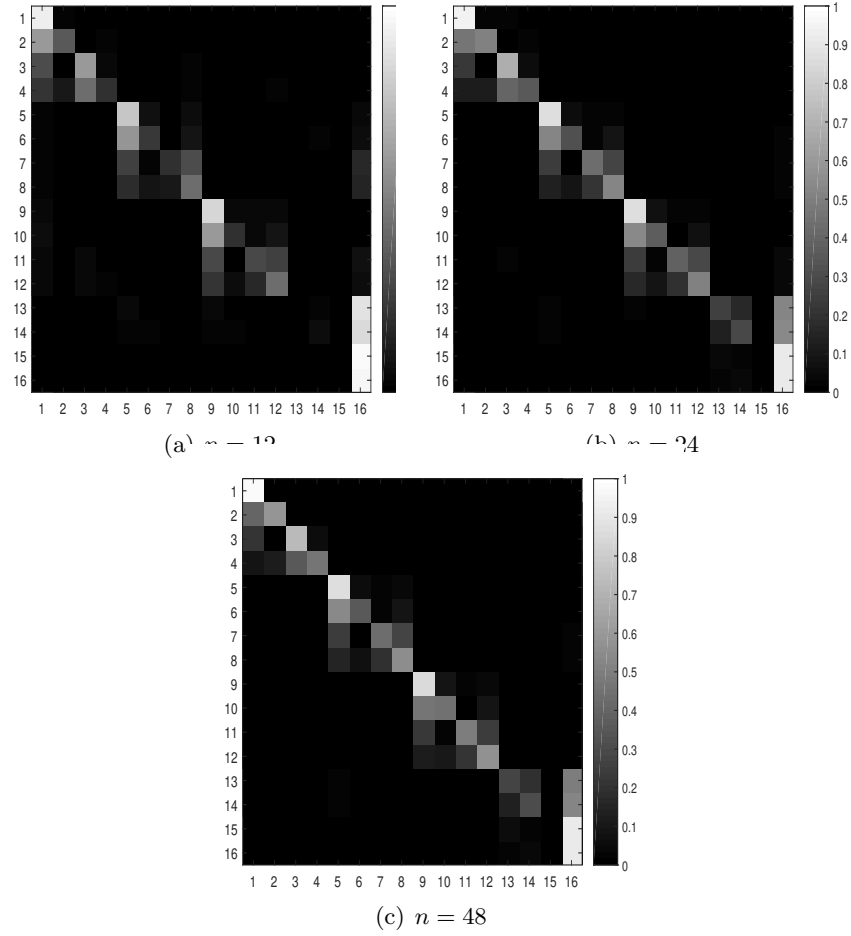


Figure 11: Misclassification matrices obtained for the *RE models* of the logistic regression example with the *unequal prior*.

Appendix C Misclassification Matrices for Epidemiological Example

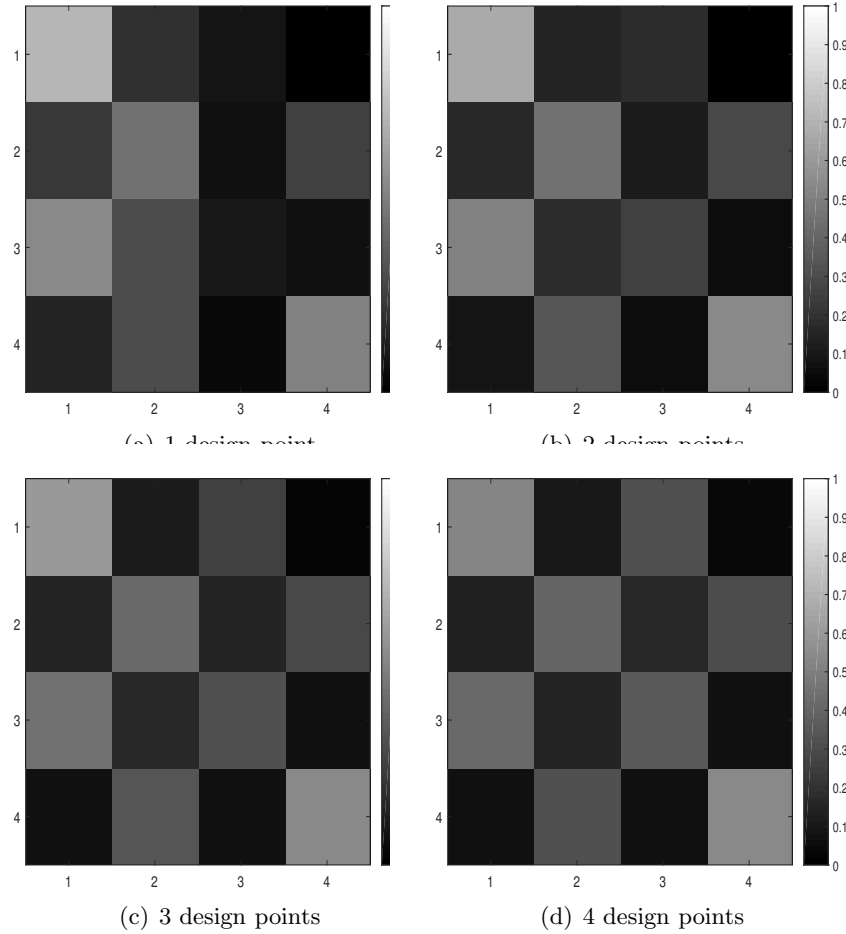


Figure 12: Misclassification matrices obtained for the *tree classification designs* (*no test samples*) under the $0-1$ loss for the infectious disease example. Designs for 1 – 4 observations are considered.

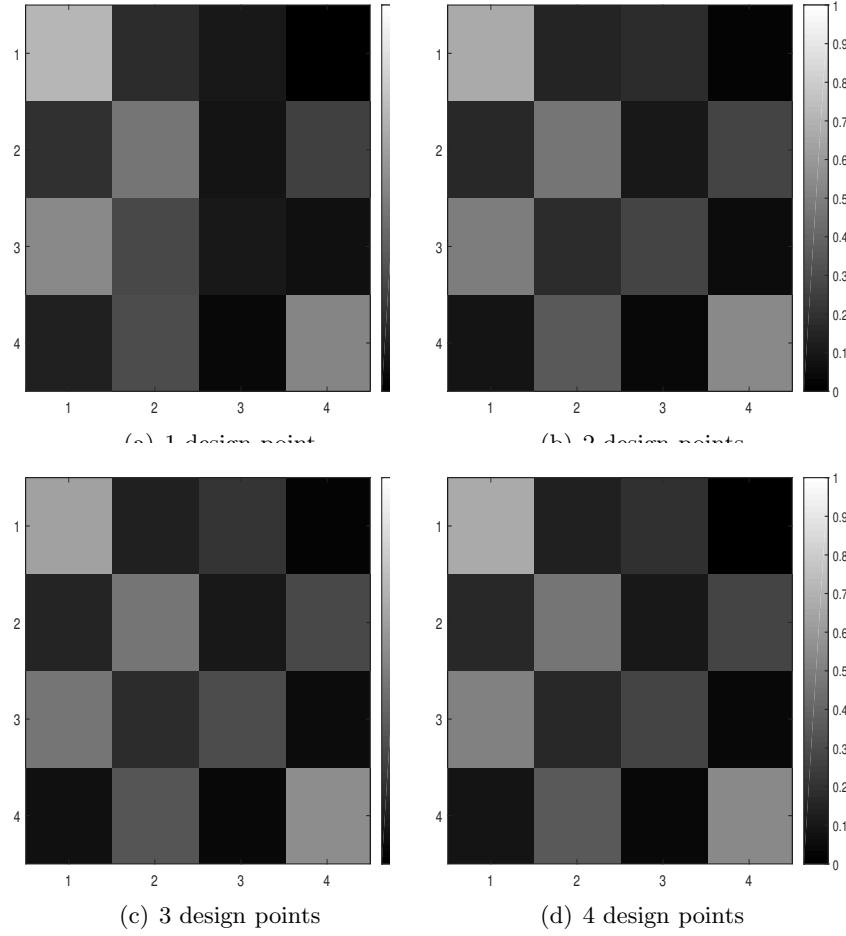


Figure 13: Misclassification matrices obtained for the *random forest classification designs* under the $0-1$ loss for the infectious disease example. Designs for 1 – 4 observations are considered.

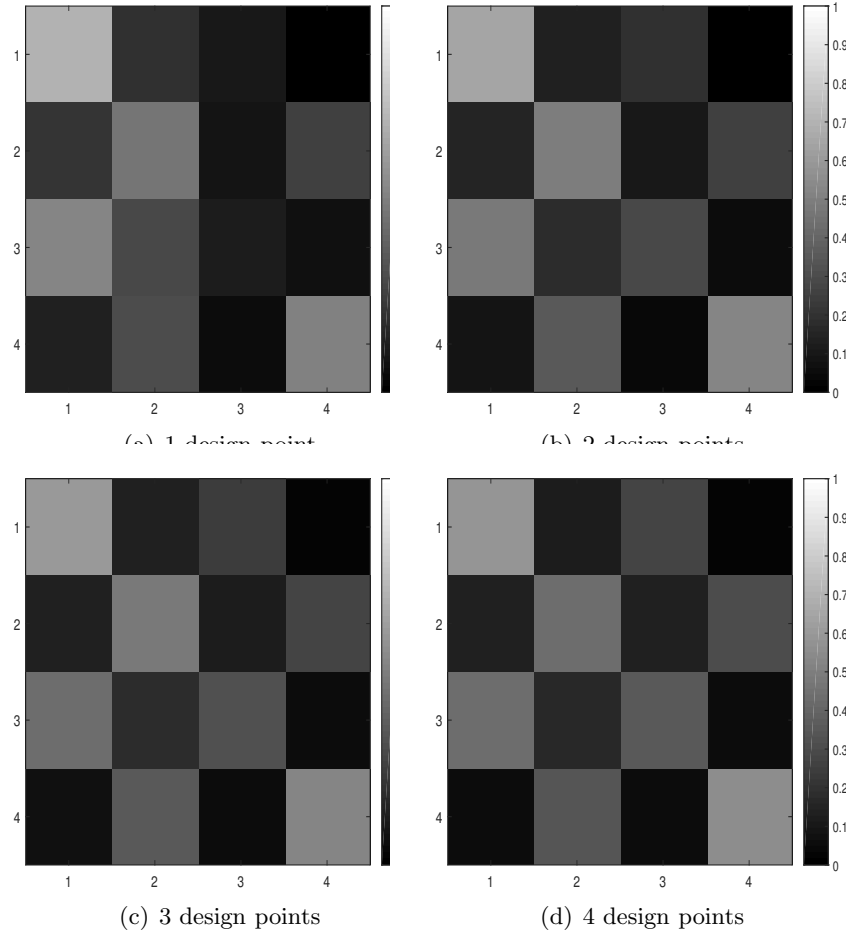


Figure 14: Misclassification matrices obtained for the *ABC classification designs* under the $0-1$ loss for the infectious disease example. Designs for 1 – 4 observations are considered.

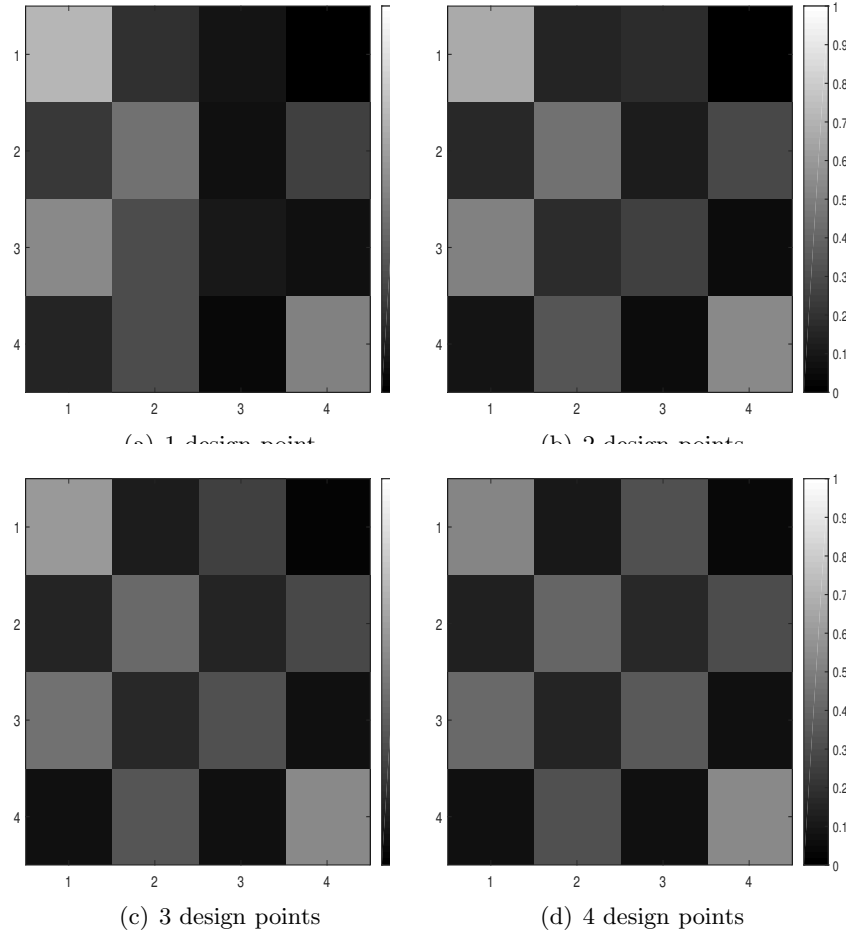


Figure 15: Misclassification matrices obtained for the *tree classification designs* (*no test samples*) under the *multinomial deviance loss* for the infectious disease example. Designs for 1 – 4 observations are considered.

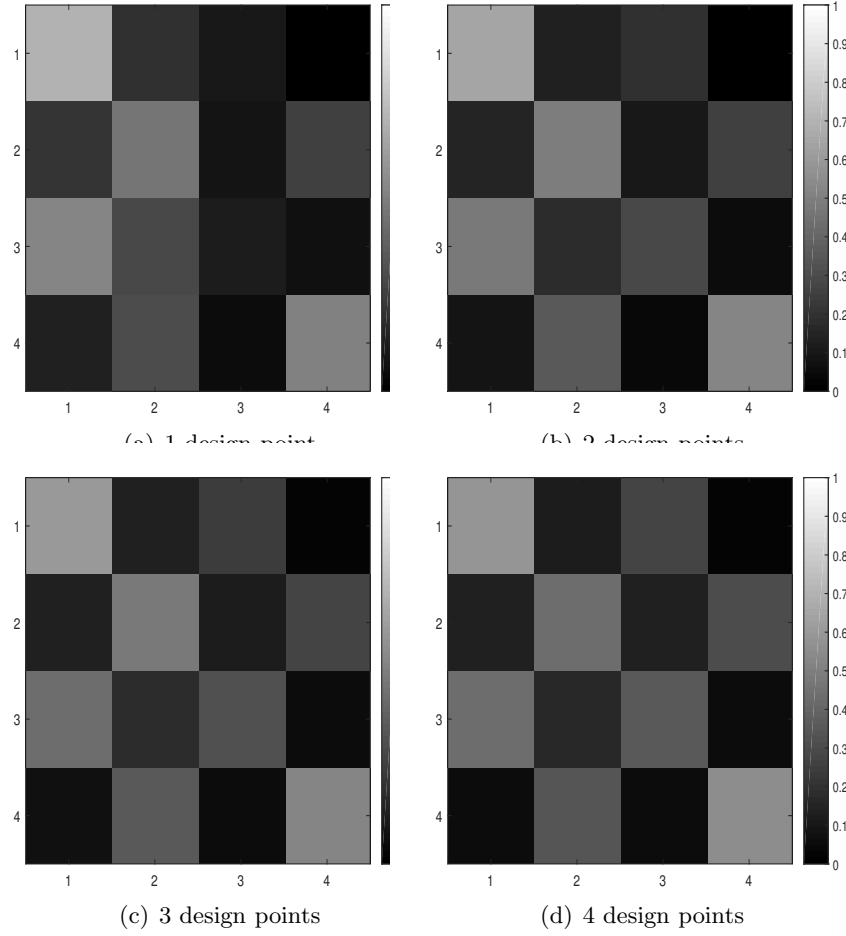


Figure 16: Misclassification matrices obtained for the *ABC classification designs* under the *multinomial deviance loss* for the infectious disease example. Designs for 1 – 4 observations are considered.

Appendix D Prior Distributions for Macrophage Example

The prior distributions for each model were driven by the analysis of the experimental system in Restif et al. (2012). We assume truncated multivariate normal distributions, where the mean vector and variance-covariance matrix are based on the maximum likelihood estimates (MLEs) and the inverse of the Hessian obtained from the optimisation routine, respectively. All parameters are truncated below at 0. The proportion parameters p and q are additionally truncated above at 1.

In model 1, all macrophages are permissive, so $q = 0$. The mean vector and the variance-covariance matrix of the truncated normal prior for the remaining parameters of model 1 are given by

$$\boldsymbol{\mu}_1^\top = \begin{matrix} & a & b & d & \delta & \epsilon & p & \phi \\ (6.46 & 1.54 & 0.073 & 2.529 \cdot 10^{-10} & 0.035 & 0.097 & 0.25) \end{matrix}$$

and

$$\boldsymbol{\Sigma}_1 = \begin{matrix} & a & b & d & \delta & \epsilon & p & \phi \\ \begin{matrix} a \\ b \\ d \\ \delta \\ \epsilon \\ p \\ \phi \end{matrix} & \begin{pmatrix} 32.8310 & & & & & & \\ 0.6224 & 0.0696 & & & & & \\ 0.1991 & -0.0017 & 0.0487 & & & & \\ 0.1258 & 0.0218 & -0.0164 & 0.0153 & & & \\ 0.0166 & 0.0048 & -0.0069 & 0.0052 & 0.0024 & & \\ 0.2142 & 0.0252 & -0.0061 & 0.0102 & 0.0039 & 0.0192 & \\ -0.0101 & 0.0001 & -0.0029 & 0.0018 & 0.0011 & 0.0018 & 0.0030 \end{pmatrix} \end{matrix}.$$

(The upper triangular part of the variance-covariance matrices is omitted.)

For model 2, where all bacteria are replicating and hence $\delta = p = 0$, the mean vector and the variance-covariance matrix are selected to be

$$\boldsymbol{\mu}_2^\top = \begin{matrix} & a & b & d & \epsilon & \phi & q \\ (8.54221 & 1.450254 & 0.09111 & 0.03 & 0.25948 & 0.266837) \end{matrix}$$

and

$$\boldsymbol{\Sigma}_2 = \begin{matrix} & a & b & d & \epsilon & \phi & q \\ \begin{matrix} a \\ b \\ d \\ \epsilon \\ \phi \\ q \end{matrix} & \begin{pmatrix} 33.5250 & & & & & \\ 1.1380 & 0.3586 & & & & \\ 0.8252 & -0.1213 & 0.0952 & & & \\ 0.0253 & 0.0077 & -0.0023 & 0.1067 & & \\ -0.1471 & -0.0511 & 0.0197 & -0.0001 & 0.0355 & \\ 0.9048 & 0.1962 & -0.0658 & 0.0097 & -0.0284 & 0.2765 \end{pmatrix} \end{matrix}.$$

Finally, model 3 assumes that all macrophages are permissive and all bacteria are replicating, so $\delta = \epsilon = p = q = 0$. For this model the truncated normal prior's mean vector and variance-covariance matrix are

$$\boldsymbol{\mu}_3^\top = \begin{matrix} & a & b & d & \phi \\ (0.8161965 & 0.52672325 & 0.20740975 & 0.3203258) \end{matrix}$$

and

$$\boldsymbol{\Sigma}_3 = \begin{matrix} & a & b & d & \phi \\ \begin{matrix} a \\ b \\ d \\ \phi \end{matrix} & \begin{pmatrix} 0.7518 & & & \\ 0.1172 & 0.0506 & & \\ 0.0720 & -0.0090 & 0.0228 & \\ 0.0008 & -0.0106 & 0.0100 & 0.0287 \end{pmatrix} \end{matrix}.$$

Figures 17, 18, and 19 contain the histograms of the univariate marginal prior distributions and the contour plots of the bivariate marginal prior distributions for models 1, 2, and 3, respectively.

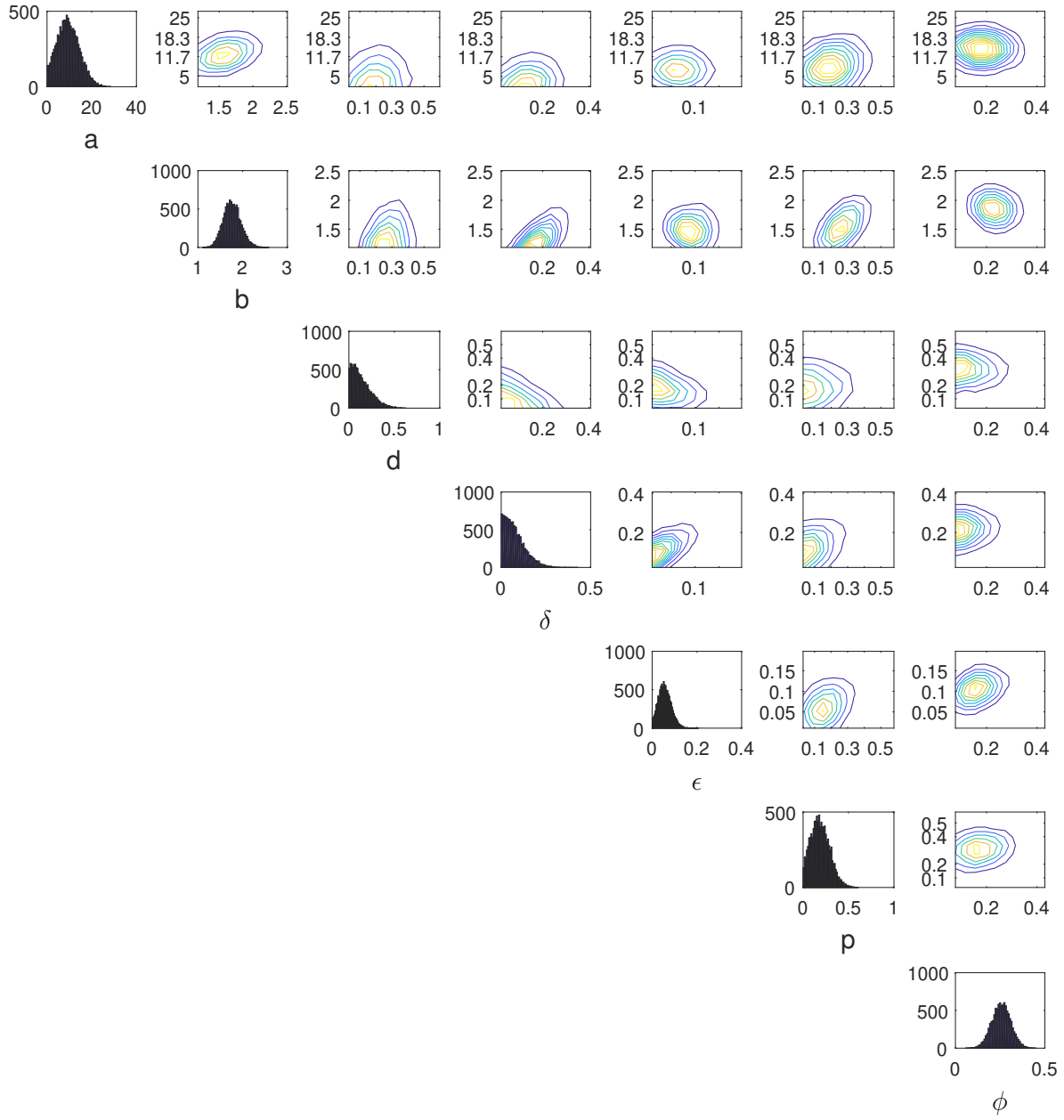


Figure 17: Histograms of the univariate marginal prior distributions and contours of the bivariate marginal prior distributions for the macrophage example's model 1 (heterogeneity in bacteria).

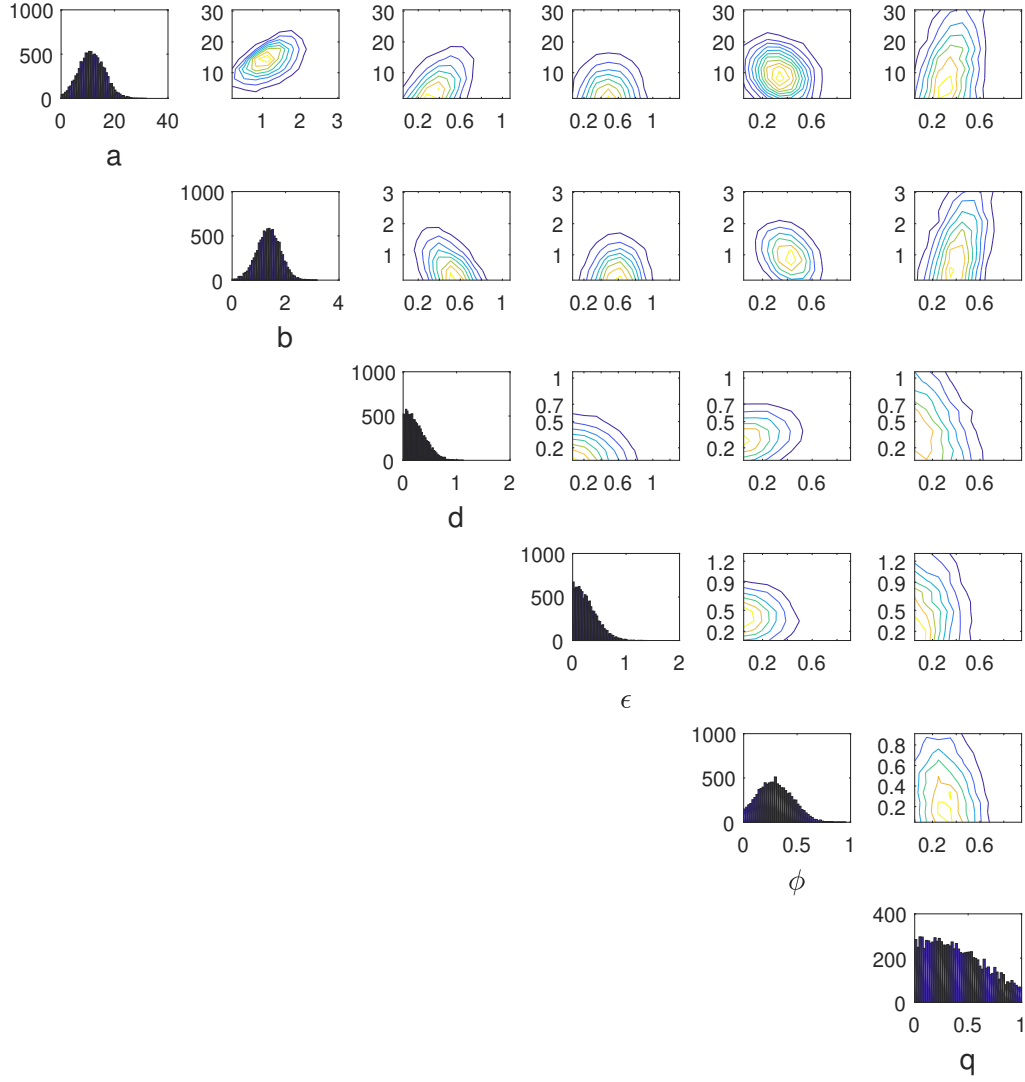


Figure 18: Histograms of the marginal parameter prior distributions and contours of the bivariate marginal prior distributions for the macrophage example's model 2 (heterogeneity in macrophages).

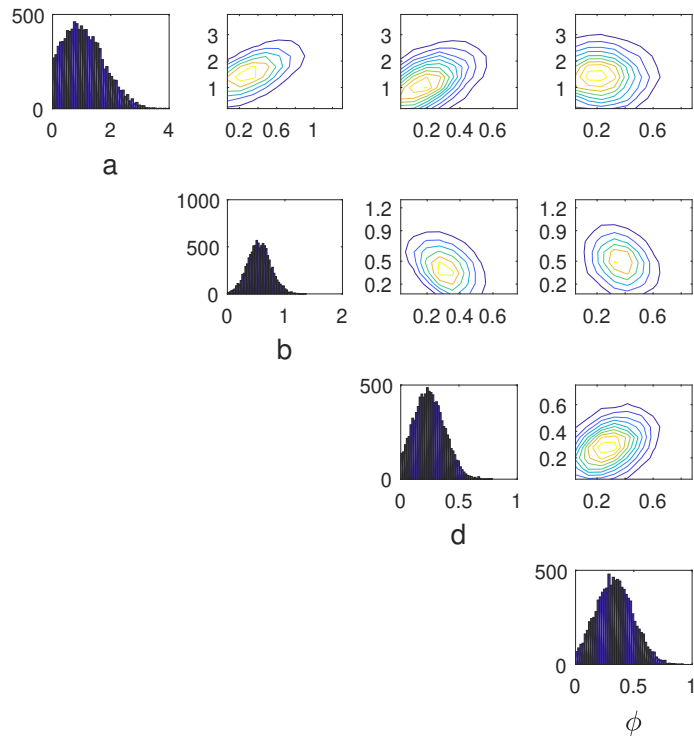


Figure 19: Histograms of the marginal parameter prior distributions and contours of the bivariate marginal prior distributions for the macrophage example's model 3 (no heterogeneity).

Appendix E Misclassification Matrices for Macrophage Example

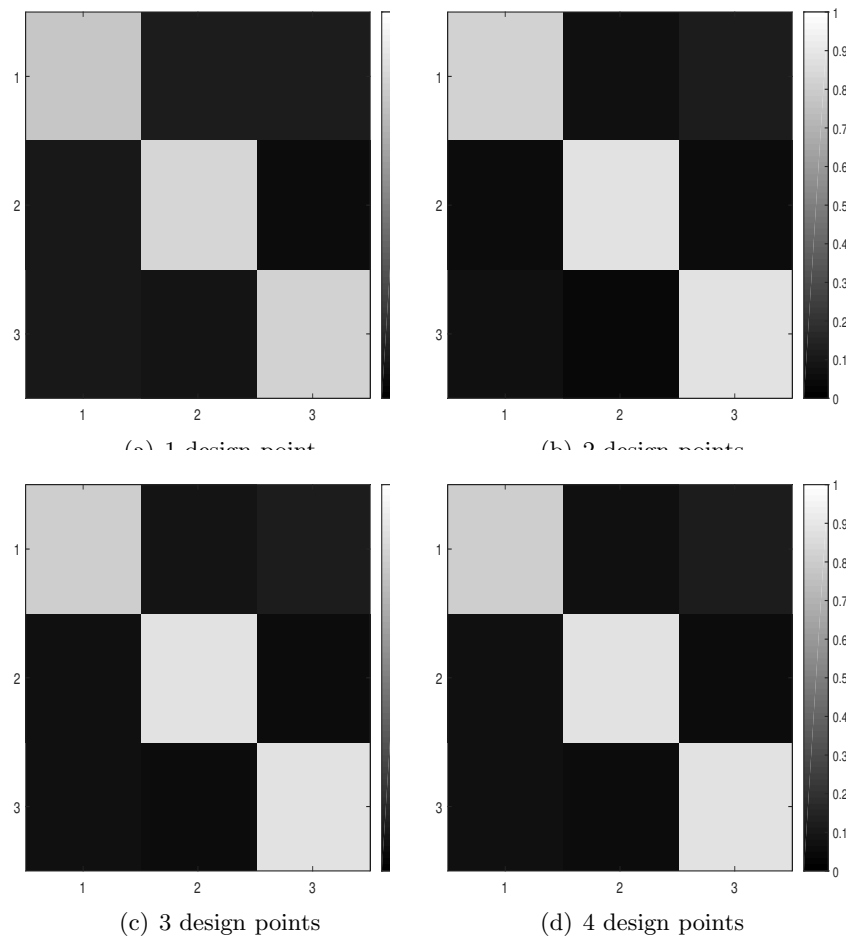


Figure 20: Misclassification matrices obtained for the *tree classification designs* under the $0-1$ loss for the macrophage example. Designs for 1 – 4 observation times plus the exposure duration are considered.

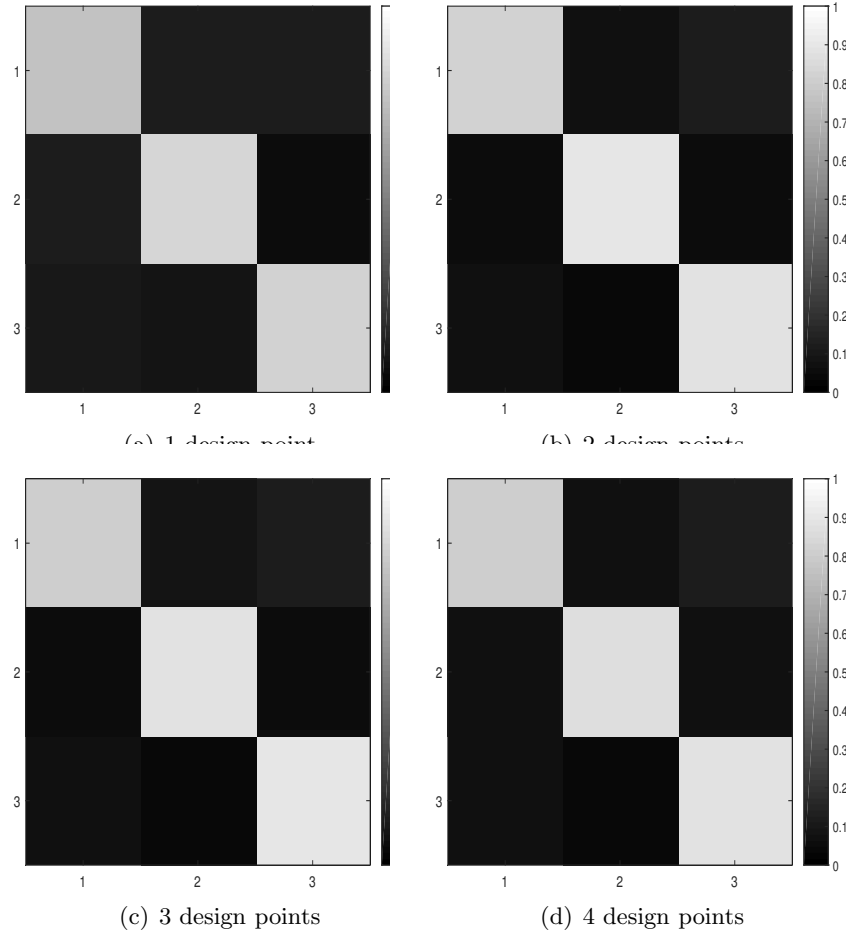


Figure 21: Misclassification matrices obtained for the *random forest classification designs* under the $0-1$ loss for the macrophage example. Designs for 1 – 4 observation times plus the exposure duration are considered.

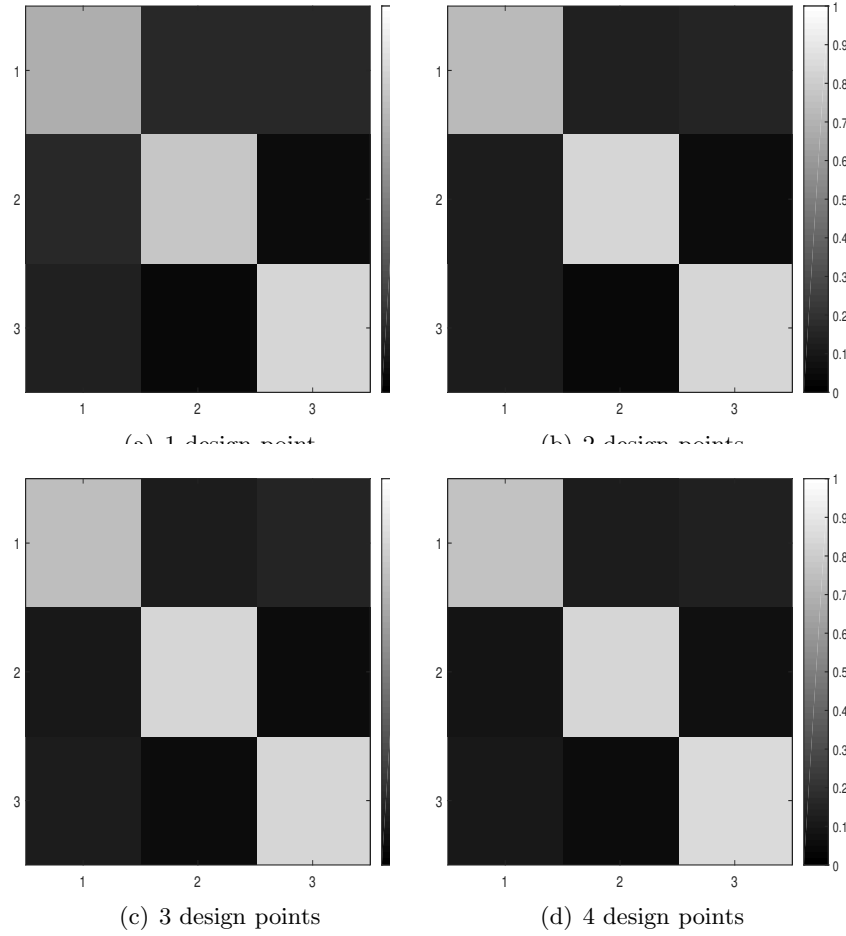


Figure 22: Misclassification matrices obtained for the *equispaced designs* for the macrophage example. Designs for 1 – 4 observation times plus the exposure duration are considered.

Appendix F Optimal Designs for Spatial Extremes Example

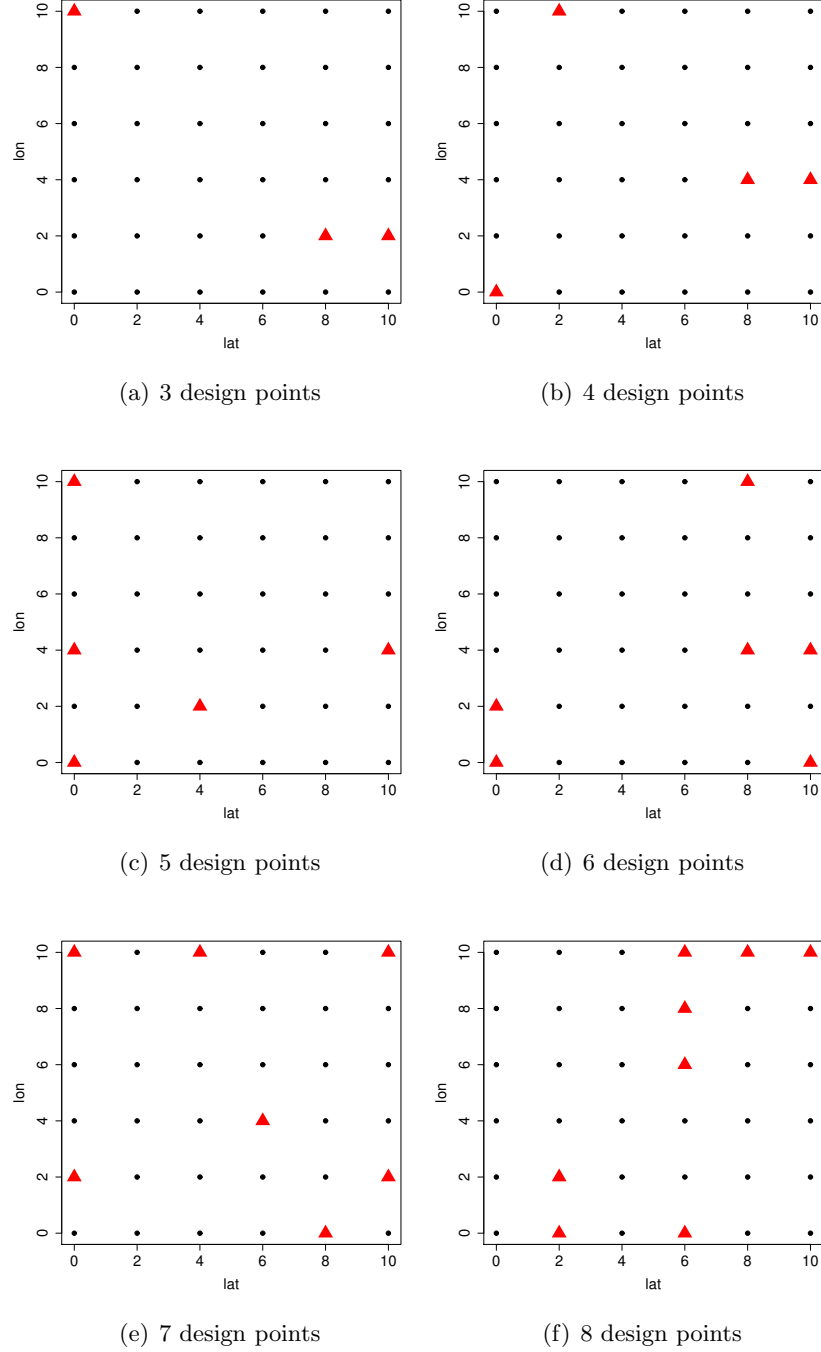
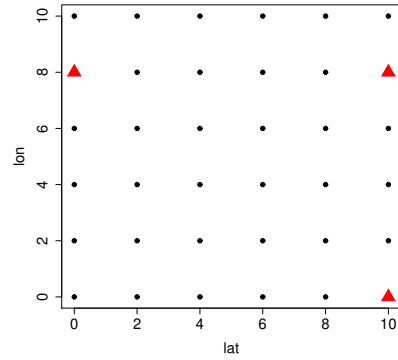
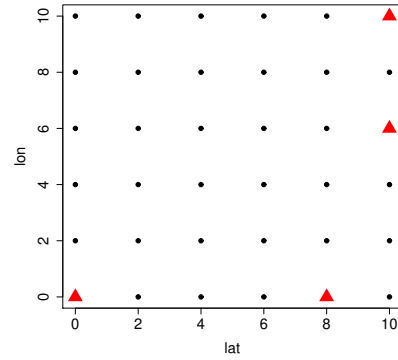


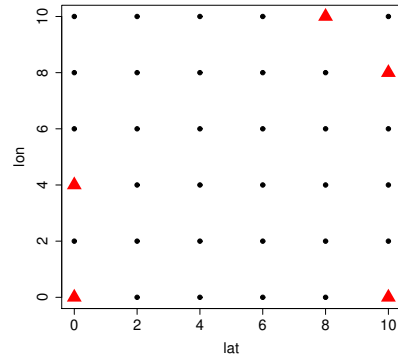
Figure 23: Optimal classification designs found using *trees* for design sizes from three to eight for the spatial extremes example. Selected design points are marked by red triangles.



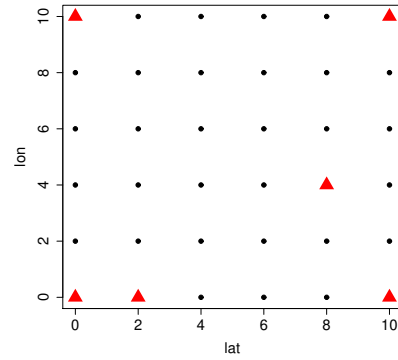
(a) 3 design points



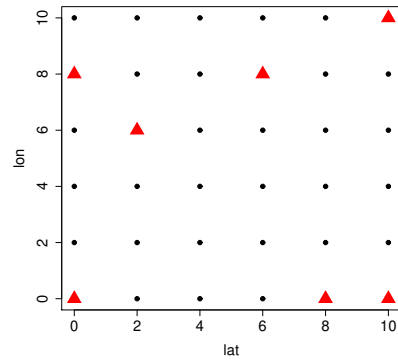
(b) 4 design points



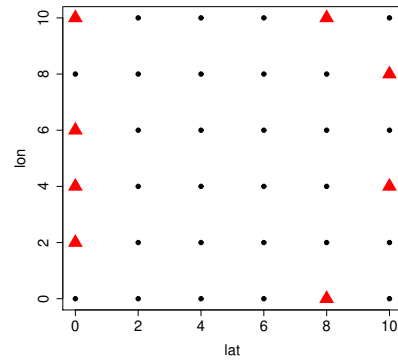
(c) 5 design points



(d) 6 design points



(e) 7 design points



(f) 8 design points

Figure 24: Optimal classification designs found using *random forests* for design sizes from three to eight for the spatial extremes example. Selected design points are marked by red triangles.

Appendix G Misclassification Matrices for Spatial Extremes Example

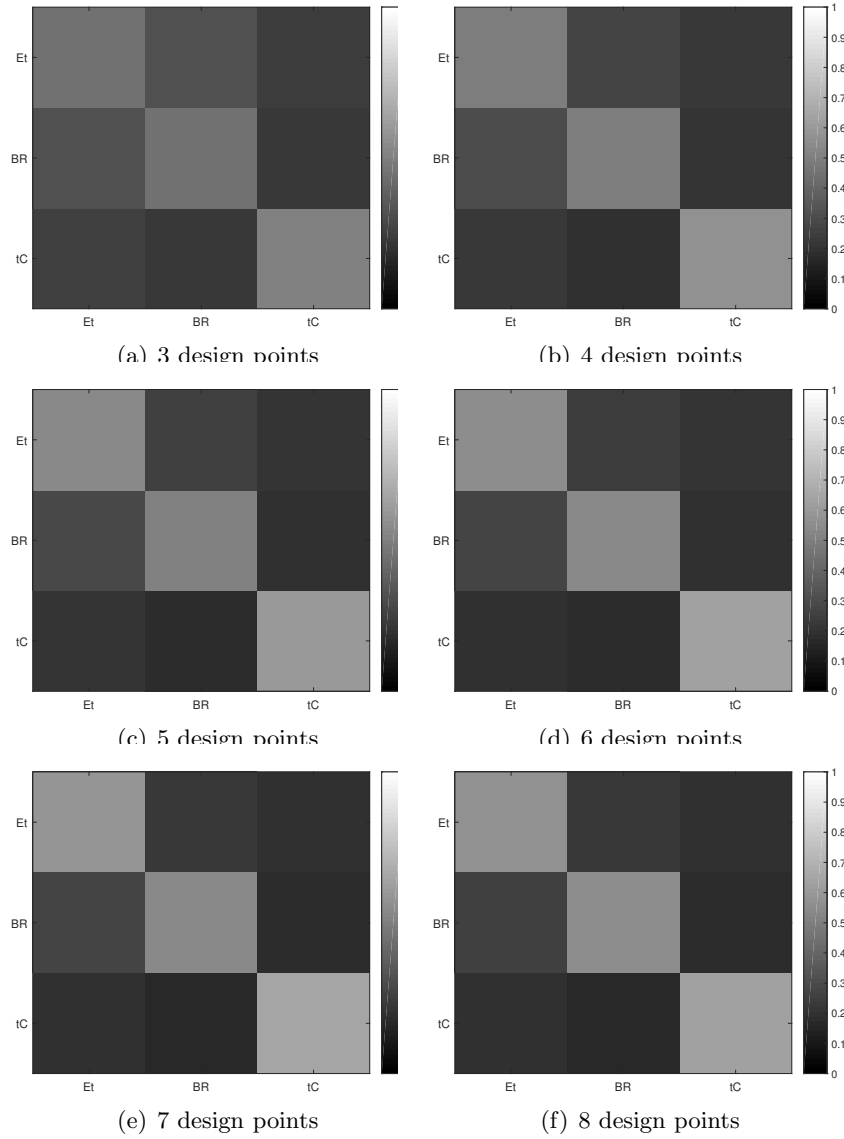


Figure 25: Average misclassification matrices over 100 simulated datasets obtained for the *tree classification designs* for the spatial extremes example. Design sizes from 3 – 8 design points are considered.

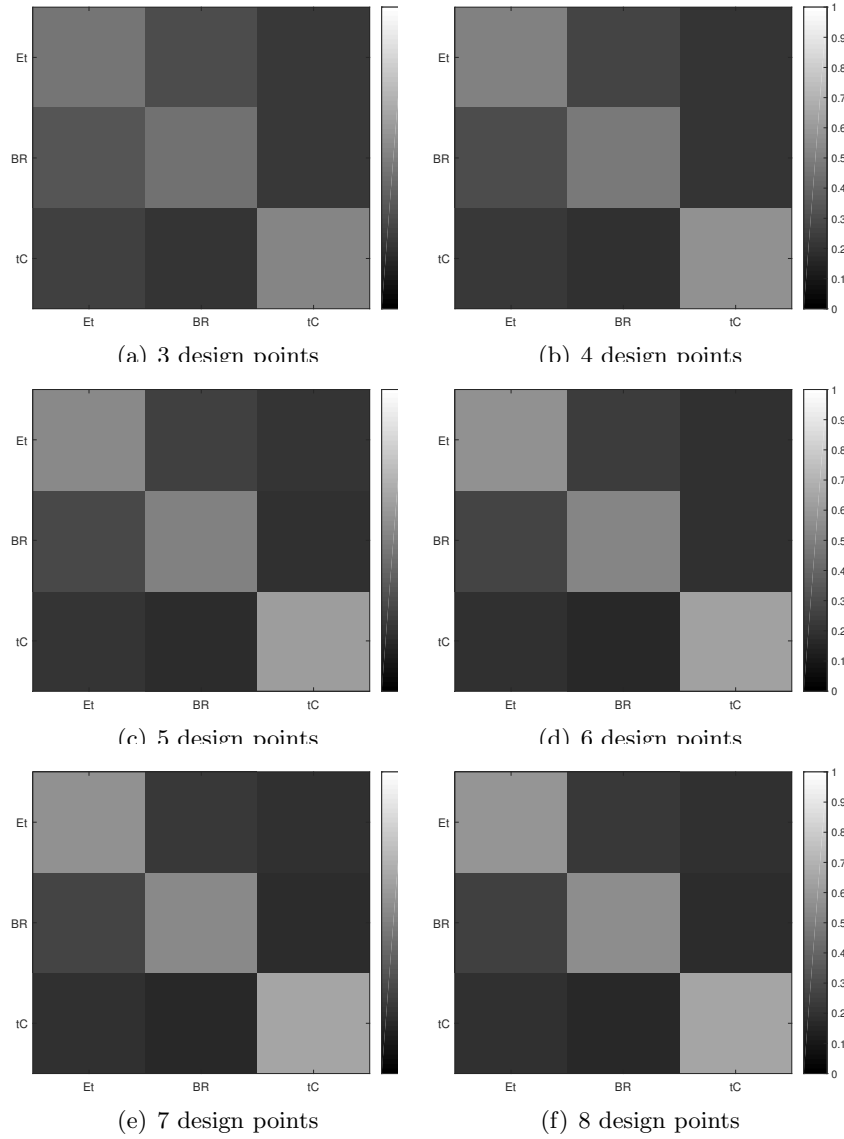


Figure 26: Average misclassification matrices over 100 simulated datasets obtained for the *random forest classification designs* for the spatial extremes example. Design sizes from 3 – 8 design points are considered.